AN EXPERIMENTAL INVESTIGATION INTO SCHOTTKY BARRIER AND METAL-INSULATOR-SEMICONDUCTOR SOLAR CELLS

BY

ABUL ISLAM MD. NAZME RAHMANI KHONDKER

A THESIS
SUBMITTED TO THE DEPARTMENT OF ELECTRICAL ENGINEERING
IN PARTIAL FULFILMENT OF THE REQUIREMENTS FOR THE DEGREE
OF
MASTER OF SCIENCE IN ENGINEERING(ELECTRICAL)

DEPARTMENT OF ELECTRICAL ENGINEERING
BANGLADESH UNIVERSITY OF ENGINEERING AND TECHNOLOGY, DACCA

AUGUST, 1980

CERTIFICATE

This is to certify that this work has been done by me and it has not been submitted elsewhere for the award of any degree or diploma.

Countersigned:

(Supervisor)

9/8/80
(Signature of the candidate)

CERTIFICATE

This is to certify that this work has been done by me and it has not been submitted elsewhere for the award of any degree or diploma.

Countersigned:

Accepted as satisfactory for partial fulfilment of the requirement for the Degree of M.Sc.(Engg.) in Electrical Engineering.

Examiners:

1. ______________________
(Professor A.M. Patwari)
Deptt. of Electrical Engineering
BUET, Dacca.

CHAIRMAN

2. ______________________
(Dr. A. Sattar Syed)
BCSIR Laboratories, Dacca.

EXTERNAL MEMBER

3. ______________________
(Professor A.M. Zahoorul Huq)
Head, Deptt. of Electrical Engg.,
BUET, Dacca.

MEMBER

4. ______________________
(Professor Shamsuddin Ahmed)
Deptt. of Electrical Engineering,
BUET, Dacca.

MEMBER

ACKNOWLEDGEMENT

The investigation reported herein was carried out under the supervision of Prof. A.M. Patwari, Department of Electrical Engineering, BUET, Dacca. The author wishes to express his sincere and profound gratitude to him for his guidance, invaluable suggestions and encouragement throughout the investigation.

Sincere gratitude is expressed to Prof. A.M. Zahoorul Huq, Head of Electrical Engineering Department, BUET, for his suggestions and encouragement at the various stages of the study. His efforts to help procure literature from home and abroad is also gratefully lauded.

The help rendered by Mr. Md. Shamsul Alam and Mr. Md. Ali Choudhury of Electrical Engineering Department, BUET, at the various stages of the work is gratefully acknowledged.

The name of Dr. W.A. Anderson of SUNY of Buffalo N.Y. USA is expressed with deep acknowledgement, for his suggestions through correspondence and for the literature he send related to this work.

The author also wishes to take the previlege of thanking his cousin, Mr. Yusuf Razee Billah, Lecturer, Civil Engineering Department, BUET and the students of Architecture Faculty for taking the trouble in the drawing and preparation of the figures.

The author also wishes to express his indebtness to Mr. M.A. Malek of Civil Engineering Department for the help rendered in typing the manuscript, and Md. Shamimul Islam for final editing and binding.

ABSTRACT

Schottky barrier and Metal-Insulator-Semiconductor has been used as a possible low cost technique for the large scale production of solar cells on thin film epitaxial silicon. These solar cells have been fabricated on p-type silicon and their physical behaviour has been derived from current-voltage (I-V) measurements. Aluminium, Chromium/Copper were used as metal contacts. Aluminium and gold were used as backside ohmic contact.

Among the different variables that are responsible for good performance, much attention was given toward the formation of oxide insulating layer over the silicon because it results in an enhancement of open circuit coltage which is essential for higher conversion efficiency. Simple methods were tried to form reproducible interfacial oxide layer using heat-treatment techniques. Investigations have also been carried out on the control of barrier heights, optical transmission and series resistance.

Computer programs were developed for the determination of the theoretical performance of the solar cells using experimentally determined values as input data. Optimisation program was also developed for the determination of the structure of current collecting grids. Indigenous methods were, however, used to form these current collecting grids.

The ideality parameters was found to deviate largely from unity. This increased value of ideality parameter was attributed to the thick interfacial oxide layer. The resistance values obtained were higher than expected due to the oxide layer and due to non optimisation of grid structures.

LIST OF SYMBOLS

A^*	Richardson's constants, $A/cm^2/{}^oK^2$
A^{**}	Effective Richardson's Constant, $A/cm^2/{}^oK^2$
C	Velocity of light, 3×10^8 m/Sec.
D_p	Diffusion constant, cm^2/Sec.
D_s	Surface states density, $/cm^2$-ev.
d_i	Thickness of different layers, cm.
E_c	Lowest energy level in conduction band, ev.
E_F	Fermi energy, ev.
E_{Fs}/E_{Fm}	Fermi level in Semiconductor/Metal, ev.
$E_{Fp}(W)$	Quasi Fermi level for holes at x=W, ev.
E_g	Band gap, ev.
E_v	Highest energy level in valance band, ev.
E_p	Energy of photon, Joules
FF	Fillfactor
f	Quantum efficiency
h	Planck's constant, 6.624×10^{-34} Joules-Sec.
I	Current, Amp.
I_o	Dark saturation current, Amp
J	Current density, Amp/cm^2
J_o	Saturation current density, Amp/cm^2
J_m	Maximum current density, Amp/cm^2
J_{mp}	Current density at maximum power point, Amp/cm^2
$J_{sm}{}^e$	Electron current density at x=0 from semiconductor conduction band to metal
$J_{ms}{}^e$	Electron current density at x=0 from metal to semiconductor conduction band

$J_e(x)$	Net electron current density at any x in semiconductor
$J_h(x)$	Net hole current density at any x in semiconductor
J_{DL}^{e}	Hole current generated by light in the depletion region Amp/cm^2
J_{Drec}^{e}	Recombination current density Amp/cm^2
J_{Difr}	Recombination current density from interface, Amp/cm^2
J_{Dunav}	Band-to-band recombination current density, Amp/cm^2
K	Boltzmann's constant, 8.62×10^{-5} $ev/^{o}K$
K_i	Dielectric constant
L_p/L_n	Diffusion length of hole/electron, cm
m_t	Cyclotron effective mass for a magnetic field in x-direction
n	Ideality parameter
N_D/N_A	Shallow, donor/Acceptor impurity concentration, cm^{-3}
n_i	Refractive index
P_{max}	Maximum power, Watt
R_j	Nonlinear junction resistance, ohm
R_{sh}	Shunt resistance, ohm
R_L	Load resistance, ohm
r_i	Reflection coefficient
T	Absolute temperature
T'_c	Fraction of solar energy transmitted
T_c	Tunneling transmission coefficient of carriers from conduction band
T_v	Tunneling transmission coefficient of carriers from valence band
t_i	Transmission coefficient
U	Total recombination rate, /sec.

V	Applied potential, volts
V_{mp}	Voltage at maximum power, volts
V_{oc}	Open circuit voltage, volts
V_R	Reverse bias voltage, volts
V_{bi}	Built-in potential, volts
W	Width of depletion layer, cm
η_{max}	Maximum efficiency
ϕ	Photon flux, photons/cm^2-sec
λ	Wave length, cm
ϕ_m	Metal work function, V
ϕ_{Bn}/ϕ_{Bp}	Barrier height of n-type/p-type semiconductor
ϕ_{Bno}	Zero field barrier height of n type semiconductor
ϕ_{Bpo}	Zero field barrier height of p type semiconductor
$\Delta\phi$	Image force barrier lower, V
ϕ_o	Neutral energy level at the surface, V
δ	Thickness of interfacial oxide layer
Δ	Potential across interfacial layer
ρ	Charge density, Coul/cm^2
ρ'	Resistivity, ohm-cm
α	Absorption coefficient
τ_p	Hole life time in bulk semiconductor region, sec.
χ_p/χ_n	Average height of potential barrier to holes/electrons tunneling between the metal and semiconductor
χ	Electron affinity of semiconductor, V

CONTENTS

LIST OF FIGURES

CHAPTER I

INTRODUCTION

1.1 INTRODUCTION

The energy crisis began to take effect from the last decade as evidenced by fuel shortage across the whole world. Solution to the energy problem has given rise to an energy debate which classifies the present technologies into two major types. One type involves huge, centralized and non-renewable sources such as nuclear and coal fired plants. With increasing demand for energy and with ever increasing cost of generation of electricity through these conventional processes, it has now become imperative to study the possible alternate, diverse and renewable energy sources. This growing demand for energy throughout the world has caused great importance to the exploration to these energy sources. Among the unconventional sources that have been studied, solar energy now holds out much promise.

The prospect of converting energy into a useful form on a large scale may sometimes seem an ecologist's dream, incompatible with the needs of modern civilization. Yet, until comparatively recent times, man relied almost entirely on the sun for his energy demands. Only in the nineteenth century the extraction of fossil fuels became important when there was a rapid growth of industry in Western Europe and the United States of America. But today, man has become aware of the increasing dangers of pollution and the limited supplies of his present non-renewable energy sources. Towards the end of this century, the conventional fuel will become scarce and expensive. It has, therefore, become important to take the advantage of the remaining time to develop solar energy system to an economic level at which they could at least solve a substantial part of the energy problem.

In this thesis considerations were given to a method that does not involve heat but converts the solar radiation directly to electrical power. This method, known as photovoltaic conversion, eliminates the intermediate step of conversion to heat and it bypasses the Carnot limitation of efficiency of heat engine. For this reason photovoltaic conversion has held out great promise in the field of direct energy conversion.

About two hundred years ago, agricultural economics utilized 'natural' solar energy. The advanced industrial societies not only need devices using solar energy in its natural state but also some apparatus to convert it into 'artificual useful form, capable of powering modern machines, and the means to store this energy so as to ensure a continuous supply. Solar cells convert solar energy directly to the electrical energy which is a very useful form of energy. Solar cells on a house roof could produce 4000 Watts using 10% efficient cells on a 20x20 ft roof and air mass 1 sunlight (100 mW/cm^2). The sun supplies 10^6 times the energy of world's present electric power capacity[39]. Ten percent efficient solar cells on 0.5% of the Sahara desert could supply the electricity consume by the entire world.

Bangladesh is a developing country. The increase in the price of conventional fuel has adversely affected its economy.

The measure of development in the present world is the energy utilized by any country. With world wide fuel shortage, it has now become very essential for this country to search for alternate sources of energy. At present our country is spending huge amount of capital in installing centralized power system. Almost all the equipment and materials are imported from abroad. Also we are to import the fuel and spares to keep the present system running. At this stage we should compare the cost of line construction and line loss to the cost of decentralized photovoltaic systems. Using low cost photo-voltatic system many houses can be self sufficient in energy. Also pumps, driers etc. can be driven from small unit generating solar electricity. Apart from slight inconsistency in rainy season in Bangladesh bright sunlight is available for most of the time of the year. But the greatest advantage of photovoltaic system in comparison to other system using solar energy is that it is able to convert energy even under diffused sunlight condition and it is possible to use the solar cell throughout the whole year.

At present the cost of solar cells is high for conventional p-n junction solar cells. Single crystal silicon technology may significantly reduce the solar cell cost. An edge-defined film-fed growth method may lower silicon processing costs 300 fold[39]. Schottky barrier solar cells (SBSC) and Metal-Insulator-Semiconductor (MIS) solar cells offer a possible solution for future application. Reduced silicon processing costs present a method for economical energy conversion.

Schottky barrier and MIS solar cells can be formed by simply depositing an Ohmic metal, depositing a transparent barrier metal and applying contact. All of these could be accomplished in a proper vacuum system with one pump-down. SBSC and MISSC offer design flexibility in the choice of barrier metals or alloy, metal thickness, antireflecting coatings. SBSC theory developed from work on single crystal can be extended to work on polycrystalline silicon for future large area SBSC[59].

1.2 HISTORY OF SOLAR ENERGY CELLS

Prior to 1953, selenium photocells were the most efficient devices that could convert solar energy directly into electrical energy with a maximum efficiency of 0.8 percent. Such a low efficiency is adequate for photographic exposure meters, but not for practical generation of electrical energy from sunlight. Yet, the desirability for a high efficiency 'solar battery' was fully appreciated at that time. At Bell Laboratories D.M. Chapin[1] was investigating electric power sources for communication systems in remote places for which it was highly desirable to use solar energy. At that time, C.S. Fuller was working on the development of various procedures for forming p-n junction by diffusion of impurities. The seemingly unrelated activities were brought together when G.L. Pearson, who studied large area p-n junctions made by Fuller method, observed that the devices were very sensitive to light. Pearson was aware of Chapin's efforts and together they tested Pearson's 'diode' in bright sunlight and observed a conversion efficiency of 4 persent.

The first devices tested by Chapin and Pearson were made by lithium diffusion into p-type silicon — an 'n on p' solar cell[1]. But unfortunately these devices were very unstable even at ambient temperatures because of high diffusion coefficient of lithium.

Fuller finally developed a boron diffusion technology with which large area 'p on n' solar cells were made that showed efficiencies as high as 6 percent.

A demonstration of the solar cells in Murray Hill on April 23, 1954 and at the annual meeting of the National Academy of Sciences in Washington DC, USA, on April 26 triggered worldwide interest in the new development.

Theoretical understanding of solar cells followed the initial announcement. First of the contributions in the early history of development in the theory of p-n junction solar cells was that of R.L. Cummerow[2]. Cummerow employed the continuity equation based upon Shockley's classical diffusion-recombination model but generalized it by the addition of an optical generation term exponentially decreasing with distance. Equations were derived for the short circuit current, the maximum power output and the efficiency. This full length paper was then followed by a letter[3] applying the theory to a calculation of conversion efficiency of the silicon p-n junction solar cell.

The second of the contributers was a letter by E.S. Rittner[4]. The letter was based upon an analytical treatment similar to Cummerow but derived new numerical results for the efficiency versus bandgap and doping concentration. It concluded that the efficiency increases with doping concentration upto the saturation solubility limit and that for a loss free case there is a maximum in the efficiency of twenty six percent at an optimum bandgap of 1.5ev. The corresponding conversion efficiency for silicon is twenty three percent. These results promptly triggered a development effort[5] on gallium arsenide solar cells. It was also pointed out that a further increase in efficiency may be realized by use of an optical collection system to increase the radiation intensity at the cell surface, a suggestion the practice of which has become feasible only very recently.

M.B. Prince published an analytical treatment in 1955[6]. He also recognized that there is a fundamental relation between bandgap of the semiconductor and the maximum achievable efficiency. Later Lofersky[7] showed the optimum energy gap to be close to 1.6ev; with about 20 percent advantage over silicon with its energy gap of 1.09 ev. Lofersky also showed that the efficiency varied for different atmospheric conditions, such as outer space and terrestrial locations and that the advantage of other materials over silicon is less for terrestrial conditions.

The interest in higher solar cell efficiencies and the improved theoritical understanding increased considerable effort in solar cells utilizing materials other than silicon. The group at RCA started and experimental programme to determine solar conversion efficiencies of various semiconductors not only on GaAs[8] but also in InP, CdTe, and CdS[9]. However, in spite of excellent development effort in these areas, until now, all significant practical applications for solar cells utilize silicon devices. In another 5 to 15 years this picture may be different, but to date, the history of practical solar cells must remain restricted to silicon devices[1].

In 1957 some problems of solar cells were better understood and efficiencies above 10 percent were reported by Pearson.[10] The first experimental application of silicon solar cell was its use as a primary power source for a repeater of the Bell system rural carrier. An array of 432 silicon solar cells capable of delivering 9 Watt in bright sunlight was mounted at the top of a pole at Americus, Georgia for a period of six months beginning October 4, 1955. The solar generated power served as a trickle charger for a 22-V nickel-cadmium storage battery. During the entire period the solar power repeater operated without failure[1].

In spite of these technical success, the approach could not compete with conventional power sources. "Had it not been the space age, the solar cells might have just become just a curiosity"[1]. It was soon realized that silicon solar cells are highly cost effective as a longterm power source for satellites since weight to be launched per watt of continuously available power is significantly less with a power source that does not require any ful or other source of stored energy.

On March 17, 1958 silicon solar cells were first used in an orbiting space satellite (Vanguard I). A radio transmitter was powered by the solar cells. It operated for about eight years before radiation damage caused it to fail[1].

As space technology advanced, a major new factor entered the solar cell technology; the need for satellites to operate at altitudes where they are exposed to significant levels of readiation. At RCA Laboratories research continued in this regard[11]. It was discovered that electron radiation damages in p-type silicon was considerably less than in n-type silicon.

As the development of communication satellites commenced, the radiation hardness become a crucial importance. Since the Van Allen Belt contains a significant flux of high energy protons, the radiation damage under proton exposure was evaluated by a group from Bell Laboratories and a group from Space Technology Laboratories[12,13]. Solar cells were exposed on a variety of cyclotrons and synchrocyclotrons covering the energy range from a few Mev. to over 100 Mev. Over the entire energy range it was found that n on p solar cells could withstand a factor of three more radiation damage before their performance was degreded to the level of p on n solar cells, a factor much less than found for electrons[11,14]. This finding implied that the minority carrier lifetime under proton radiation degrades at the same rate in p and n type material, but that the factor of three higher mobility of electron minority carriers in p-type material compared to holes in n type material permits the minority carrier lifetime in n on p cells to degrade a factor of three more before equal diffusion lengths are achieved.

Since short-wave length light is absorbed close to the surface of the solar cells, and since only the collection of carriers from the bulk are affected by radiation damage, further improvements in radiation hardness were achieved by the development of 'blue' sensitive solar cells requiring very shallow diffused n layer with good surface properties and carefully designed antireflection coatings[1].

The first satellite equipped with such improved n on p solar cells was the Telstar satellite launched on July 10, 1962[15]. It changed the direction in solar cell technology to n on p solar cells for all space applications. Many satellites since then have used radiation tolerant cells and have operated for long periods of time. More recently efforts at COMSAT Laboratories led to increases in efficiency through the development of a 'violet cell', which has very high short wavelength collection efficiency by employing $\frac{1}{4}$- μ diffused layer and Ta_2O_5 anti-reflection coatings[16]. Further improvements led to cells with near zero reflectivity (black cell), increasing efficiency about 15 percent in outerspace[17]. The same cells give conversion efficiency of 17 percent - 19 percent on the surface of earth, depending on air mass and meteorological conditions.

1.3 BRIEF LITERATURE REVIEW

The advent of the energy crisis developed a renewed interest in terrestrial application of solar cells. For this energy to be economically viable, the cost of solar cells will have to be reduced by at least a factor of 100 below the cost for solar cells used in space applications. Metal-semiconductor junction or Schottky barrier silicon solar cells (SBSC) offer a possible solution for future applications. Reduced silicon processing costs present a method for economical energy conversion. The Schottky barrier solar cells are, however, primarily Schottky barrier diodes using optical biasing.

The metal semiconductor rectifier or diode is known to be the oldest solid state device used in Electronics. Braun[18] in 1874 first reported the asymmetrical nature of conduction between metal point and crystal like lead sulphide. In 1906 Pickard[19] took a patent for silicon point contact rectifier and in 1907 Pierce[20] fabricated diodes by sputtering metal to different semiconductors. In 1931 Wilson[21] formulated the transport theory,but the correct physical model was forwarded by Schottky[22] in 1938 and hence the name Schottky diode. In the same year Mott[23] devised an appropriate model for sweptout metal semiconductor known as Mott barrier. Bardeen in 1947[24] showed that if a contact is made between metal and semiconductor, the difference in work function between the two is compensated by the surface states charge, rather than by a space charge as was originally assumed, so that the space charge layer is

In 1966 Crowell and Sze(29) combined the thermionic emission theory (T) and Schottky diffusion (D) theory into a single thermionic diffusion theory (T-D) which included the image force barrier lowering effect. At the same time Mead(30) published a review paper on Schottky barriers. A qualitative explanation of the type of contact to be expected at an arbitrary metal-semconductor interface was presented in his paper.

In 1968 Turner and Rhoderick(31) found the barrier height of a number of metal conducts to n-type silicon. They showed that initial values of barrier heights depend upon the methods of surface preparation and these values changed slightly with time. They showed that the final value of barrier height was independent of surface preparation and depended mainly upon the metal work function. However, in the case of diodes where depositions were made on cleaved surfaces, the barrier height did not show any ageing.

In 1971 Smith and Rhoderick(32) found that barriers with p-type silicon were generally lower than those with n-type. Gold barriers were so low that it was apperently Ohmic. The ideality parameter was found to be about 1.1. The variations of barrier height with metal work function indicated that the surface states parameters were primarily responsible. Crowell and Beguwala(33) calculated the ideality parameter, n, and short circuit current density, Jsc, using parabolic band bending. It was found that the quasi-Fermilevel in both forward and reverse bias was discontinuous at the interface. Under moderate bias the electron imref was nearly constant throughout the depletion region. But in the case of reverse bias the imref deviates from constancy for applied bias in excess of KT/q. In 1971 Card and Rhoderick[34] made a theoretical and experimental study of silicon Schottky diodes in which the metal and semi-conductor are separated by a thin interfacial oxide film. A generalized approach was taken towards the interface states which considers their communication with both the metal and the semiconductor. Amount of current was explained by a transmission coefficient which was also a function of thickness of interfacial layer. In the same year Card and Rhoderick[35] established restriction upon the interfacial oxide thickness for which thermal equilibrium in the semiconductor is a valid approximation under the application of reverse bias.

In 1974 Patwari and Hartnagel[36] studied damaged surface Schottky barriers. Their aim was to find whether any economy could be achieved with surfaces of semiconductor whose surfaces were slightly damaged. Result showed that damage reduced the barrier height along with slight increase of ideality parameter.

Alam[37], in 1978 developed methods to control the barrier height by heat-treatment techniques. Control of barrier height in higher range was also obtained by deposition of aluminium and gold in succession on silicon. Freshly prepared barrier showed different values under different conditions which revealed that fixed positive charges were present at metal-semiconductor interface.

Schottky barrier devices were first used as solar cells in the early 70's.

In 1972 W.A. Anderson and A.E. Delahoy[38] fabricated Schottky barrier solar cells (SBSC) by evaporation and sputtering of Al, Cr, or AuCr alloy barrier metals on p-type silicon. Efficiency of 4.8 to 12 percent was reported. They also carried out some computer studies on the optical transmission problem and suggested that the barrier metal thickness should be kept between 275 to 100 Å. In 1973 Anderson and Delahoy[39] studied the theoretical and experimental considerations of the processing steps, and reflection coating and contact design to fabricate an efficient and economical SBSC.

Minority carrier metal Insulator-Semiconductor (MIS) diodes were studied by Green et el[40]. It was shown that such minority carrier MIS tunnel diode with very thin insulating layers possesses properties similar to p-n junction diode including exponential current voltage characteristics which approach the'ideal diode' law of p-n junction theory. It was also indicated that these diodes have application as energy conversion devices employing photovoltaic effects.

Pulfrey and McQuat[41] calculated the maximum theoretical solar conversion efficiency of Schottky barrier solar cells and showed that the efficiency of SBSC is very similar to that of convensional homojunction solar cells, e.g, values of 22-24% apply to silicon and 25% to semiconductors having a band gap between 1.4 and 1.6 ev. With p-type silicon the maximum efficiency can be 24.4%. In the above calculation the effective Richardson constant A^{**} was taken = 30 A cm^{-2} $^{o}K^{-2}$. In 1974 Anderson et el[42] fabricated an 8.1% efficient 1-cm^2 Schottky barrier solar cell using a layerd Schottky barrier on p-type silicon. This layered concept produces high conversion efficiency by permitting independent control of barrier height, optical transmission and series resistance. They have also investigated[43] the effect of series resistance on fill factors. Their experiment showed a significant increase in open circuit voltage with diode quality factor but with no appreciable influence on fillfactor. In these works the Schootky metal was a film of chromium. A thin layer of Cu and Cr decreased the resistance of the cells. Open circuit voltages V_{oc} = 0.52 volts and Short circuit current density J_{sc} = 30 mA/cm^2 was obtained.

In the early days of 1970's it was thought that SBSC would offer a possible solution for cost effective photovoltaic energy converter. However, it was soon realized that the performance of MIS cells is better because by introducing an oxide interfacial layer it is possible to obtain higher open circuit voltage. In 1975, Fonash[44] made a theoretical study on the role of interfacial layer in metal-semiconductor solar cells. It was shown that the interfacial layer can enhance the performance and an outline for optimizing that enhancement was presented.

Stern and Yeh[45] fabricated a 15% efficient antireflection coated metal-oxide-semiconductor (AMOS) solar cells. They developed a new effect, a marked increase in open circuit voltage, by addition of an oxide layer to the semiconductor.

Charlson and Lien[46] reported a MOS photovoltaic diode, consisting of aluminium on p-type silicon. In this device a very thin SiO_2 insulator of the order of 20-40 Å was grown on the surface of p-type silicon. Prior to deposition of an Al metal. The efficiency was 8% and height of the barrier was as high as 0.85 ev, approximately twice as large as that for the normal Al p-type silicon diode. High reflection loss of aluminium was avoided by applying a double-layer coating of zinc sulphide and silicon monoxide.

Lillington and Townsend[47] carried out measurements of the electrical and optical properties of Au-n-type silicon Schottky barrier solar cells in which the metal and semiconductor are separated by a thin interfacial oxide layer, 10-23 Å thick. Measurements of the V-I characteristics showed that the value of open circuit voltage is increased by up to 38% and the maximum conversion efficiency by asmuch as 35% when compared with cells having no grown oxide layer. Pulfrey[48] presented calculations which indicated that the barrier height of metal-thin insulator-p-silicon diodes can be greatly enhanced by the presence of positive charge in the interfacial layer. He also showed that this positive charge advantageously modifies the barrier height for p-type material and for this reason solar cells utilizing p-type materials are more sauccessful then those which utilize n-type material.

Card and Yang[49] have shown that the increases in open circuit voltage of MIS Schottky barrier solar cells due to the interfacial layer can only be understood by taking proper account of the behavior of the interface states under illuminated conditions of the cell. Interface states in the solar cell communicate most readily with the minority carriers and as a result act to reduce the potential drop in the interfacial layer, in contrast to their effect in dark forward biased diodes. They suggested that the increase in open circuit voltage cannot be explained in terms of an increased value of ideality parameter 'n' for the dark current; It can be explained from the effect of interfacial layer on the tunnel coefficient for the majority carriers. The theory predicts an optimum thickness for the interfacial layer above which the short circuit current (minority carrier current) decreases, and the efficiency (fillfactor) is degraded.

Anderson et al[50] fabricated SBSC on 10,20,30 um epitaxial silicon which produced a current density ranging from 10-22 mA/cm^2 depending on Silicon thickness and orientation which is in close agreement with theoretically predicted data. Data reported herein predicted that 10% efficient Schottky solar cells could be produced by using about 20 u of silicon on a suitable substrate. A 7.6% efficient Schottky solar cell on epitaxial silicon had been fabricated and was tested using AMI sunlight.

Anderson, Kim and Delahoy[51] reported that analysis of data on many different solar cells shows that open circuit voltage may be controlled by chromium deposition rate which modifies the sheet resistance of the Cr Schottky metal. This result suggested a change in basic structure of the Cr which leads to an apparent lowered work function ϕ_m. A lowered ϕ_m is attributed to slow deposition of Cr on an oxide substrate. It was predicted that with decreased ϕ_m and increased thicknees of oxide layer ∂ V_{oc} will increase. It was however, assumed that ∂ is large to cause the lowered ϕ_m. Experimental data on Cr-oxide-p-Si device violate the theory of Lillington and Townsend[47] in that a low n-value device may still have a high open circuit voltage V_{oc}. The theory of Card and Yang[49] predicts that V_{oc} increases with increased ∂. Fonash predicts an effective reduction of ϕ_m due in part to fixed charge in the oxide. An application of his theory agreed in principle with the result. AM1 efficiency values of these solar cells were 6-9.5% measured on 1-2 cm^2 cells.

Shang S. Li[52] made a theoretical study for novel Au-p-n-GaAs Schottky barrier solar cells. The results show that the barrier height equal to the energy band gap of GaAs can be obtained in the proposed cell structure if the thickness and the dopant density of the p-GaAs are properly choosen.

Anderson et al[53] reported that Cr-MIS solar cells having a 2 cm^2 area have been fabricated to produce 12.2% efficiency on single crystal and 8.8% efficiency on polycrystalline silicon. The dependence of the short-circuit current density on minority carrier diffusion length, and on the thickness of the Cr-Schottky layer was also investigated. Surface-state data were used to predict open circuit voltages of 0.60 and 0.50 volts for single crystal and polycrystalline Si respectively. Spectral response measurements and Cr metal thickness confirm differences in short circuit current density using these two types of silicon.

Lue and Hong(54) studied the dependence of photocurrent of MIS solar cells on the thickness of Schottky barrier metals. A theoretical study was done to calculate short circuit current. By using Fuchs-Sondheimer's(55,56) theory to calculate the electrical resistivity in thin metal films and Handy's(57) approach to calculate the series resistance on a given configuration of the contact grids, it was shown that the optimum thickness which gives the maximum short circuit current closely depends on the intensity of the illumination light and on the series resistance of the device. The optimum thickness shifts towards thicker film as the illuminating light or the series resistance increases. Fabrication of these devices on MIS solar cells indicate that the monitored optimum thickness agreed satisfactorily with theoretical value.

Pulfrey(58) presented calculations which indicate that, for a given series resistance, fillfactor is principally determined by the saturation dark current, rather than the diode factor. It was clearly shown that for a given diode factor n, increasing series resistance R_s shortens the horizontal segment of output I-V curve but does not affect V_{oc}, therefore, fillfactor decreases. It was also shown that for a constant value of n and for any value of R_s less than resistive limits increasing I_o decreases both V_{oc} and the horizontal segment of the I-V curve and so the fill factor decreases rapidly.

Pulfrey[59] in his review paper presented an excellent discussion on MIS solar cells. The efficiency of the solar cell is a function of short circuit current I_{sc} open circuit voltage V_{oc}, and fill factor, FF. Thin oxide layer enhances the open circuit voltage and the maximum value was 0.63 volts, obtained for GaAs cell and the maximum value of I_{sc}= 28.3 ma/cm^2 was achieved for silicon cell. A comparison of performance of GaAs and Si MIS cell are given in his paper. The effect of different thickness of barrier metals on the performance of cells and their properties were also tabulated. All the factors affecting these properties are explained along with suggestion for improvement of performance limiting parameters.

RajKanan and Anderson[60] investigated the current conduction mechanism in Cr-SiO_x-(p-Si) MIS solar cells. Their study demonstrated that majority-carrier tunneling over the combined barrier due to interfacial oxide layer and the space charge region dominates the I-V characteristics at room temperature. Majority carriers tunneling via interface states control the characteristics at higher temperature for these devices.

RajKanan et al[61] studied the ultra thin interfacial layer between a semiconductor and a metal contact in details. They found that since the oxide layer thickness is comparable to the nonstoichiometric transition layer, the pin-hole associated with the ultrathin layer will affect the performance of MOS solar cell. The experimental results of open circuit voltage as a function of oxide thickness for Al-SiO_x-(p-type) Si solar cells have been explained by a composite model which treats the pinhole areas as Schottky junctions and assumes a Gaussian distribution of pin holes.

1.4 SCOPE OF THE THESIS

The purpose of this thesis is to investigate the fabrication process of Schottky barrier and Metal-Insulator-Semiconductor Solar cells. Schootky barrier and MIS solar cells are being studied as a possible low cost techniques for producing thin film solar cells. Investigations were carried out on the control of barrier height, optical transmission and series resistance of these cells. Among different variables that are responsible for good performance, much attention was given towards the formation of oxide layer over the silicon because it results in an enhancement of open circuit voltage V_{oc} which is essential for higher conversion efficiency.

So far, MIS solar cell has emphasized enhancement of V_{oc} but attainment of high value of short circuit current density was by no means obvious. Simple methods were tried to form reproducible interfacial oxide layer using heat treatment techniques. Investigations were also carried out to form thin insulating layer so that photocurrent suppression effects (i.e. decreasing tunnel transmission coefficient or increasing series resistance) are avoided.

A theoretical formulation on this subject is given within the first three chapters — of which Chapter-1 deals with the brief account of some of the works done in the field of Schottky barrier diodes and solar cells. Chapter-2 gives an introduction to photovoltaics. It also deals with the theoretical consideration for the fabrication of Schottky barrier and MIS solar cells. Theory of Schottky barrier and MIS solar cells are included in Chapter-3. Fabrication process and measurements are given in Chapter-4. All the results are summarized in Chapter-5. This chapter also includes a discussion on all the important and related factors governing the performance of the fabricated solar cells. Conclusions and recommendations on future research in this field has been given in Chapter-6.

CHAPTER II

THEORETICAL CONSIDERATIONS FOR THE FABRICATION OF SOLAR CELL

2.1 PRELIMINARIES

The photovoltaic effect is a process by which a voltage is produced at the junction of two different materials, e.g., a metal-semiconductor contact or a p-n junction, through an incident photon flux. In this chapter the production of electrical power by exposing to electromagnetic radiation has been discussed. A review of radiation principles has been presented. The process of conversion has been discussed and a simple equivalent diagram has been derived. A calculation of solar cell performance on the basis of this equivalent circuit has also been included. A brief theoretical consideration on the power output and efficiency has been given. A detailed expression for different contributions to the series resistance has been shown. A computer program for the optimization of grid structure has been developed.

2.2 PHOTOVOLTAICS

The direct conversion of sunlight into electrical energy is achieved by means of 'solar batteries' made of solar cells. The process which is responsible for this conversion is known as photovoltaic effect. The term was adopted to differentiate between the photovoltaic effect and the photoconductive effect, both of which are photoelectric effects which occur in semiconductor matter. In the photo conductive effect, free charges are generated by internal ionization of the atoms or ions which constitute the semiconductor crystal when photons of light are incident upon the matter. The new mobile charges increase conductivity of the substance but this effect does not generate power because electric power is the product of voltage and current. The photovoltaic effect, on the other hand, can occur only when a potential barrier exist in the unilluminated semiconductor. Such a barrier is found, for example, at the interface between two areas of different doping, metal and semiconductor junction. If this material is illuminated, the electric charges created by light through the photo conductive effect will be separated by the barrier into positive charges on one side and negative charges on the other. This is the photovoltaic effect by which an electric power is generated. It should be noted that this kind of conversion process does not at all depend on heat. In fact, the efficiency of the solar cell device drops when its temperature rises. The fact that the photons of solar light transfer their energy directly to electrons without an intermediate thermal step has made solar cells not only appropriate in sunny regions, but seem promising for areas in which other kind of solar energy systems appear completely hopeless. Under over cast skies, concentration devices such as are utilized for the thermodynamic conversion of solar energy can not work and the efficiency of flat plate heat collectors falls to very low values. Solars cells, however, operate at the same efficiency under cloudy skies as they do in bright sunshine.

The photovoltaic conversion effect is generally achieved in all semiconductors. Insulators are unsuitable because of their high resistivity and metals are insensitive to light.

because of their high electron concentration in the dark.

Solar cell research and development has been expanding rapidly in the past few years spurred on mainly by the potential use of these cells for large scale terrestrial solar energy applications. The semiconductors which are best suited to the conversion of sunlight are the most sensitive ones, that is which give the highest current-voltage product for the visible light. In fact the largest amount of energy transmitted by the sun's rays is within the visible light parts of the spectrum. Semiconductors like Pbs are sensitive to infra-red light are therefore unsuitable for energy conversion. ZnS have maximum sensitivity in the ultravoilet part of the solar radiation spectrum and is also unsuitable. At present silicon is the most important semiconductor material for photovoltaic energy conversion and today all the cells are manufactured from monocrystalline material although there are some research going on polycrystalline structure.

All the solar cells have several things in common. There is a semiconducting layer known as the base. It has an ohmic or injecting contact on the one side and an electrostatic potential energy barrier on the other side formed by a p-n junction, a thin metal film Schottky barrier, or a heterojunction. A contact grid or finger pattern is applied to provide a low series resistance and an antireflection coating is applied to reduce the reflection loss of sun light. Encapsulation may be added to protect the cell from environment. Different solar cells may

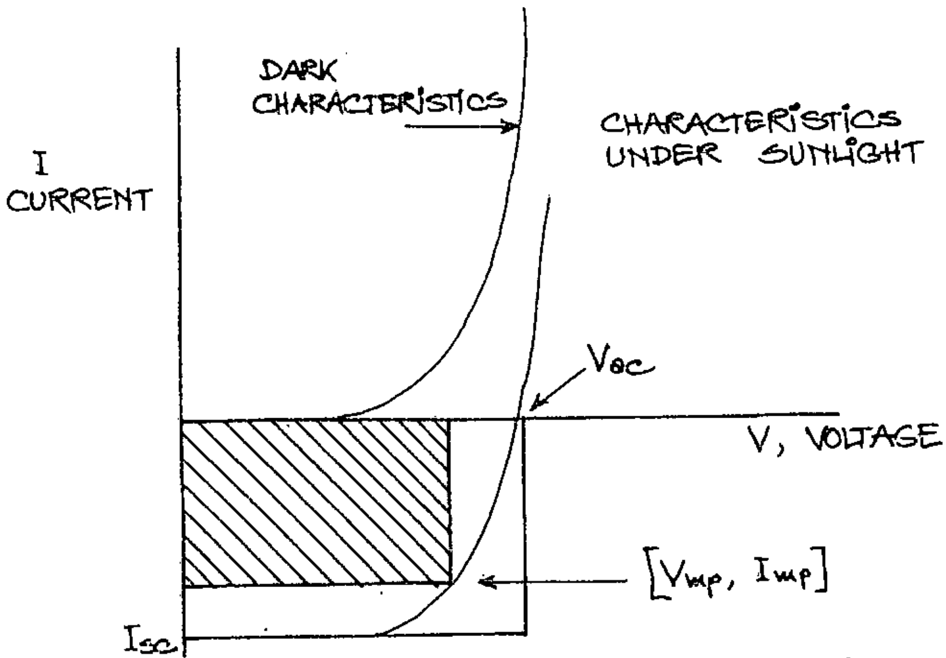

FIGURE 2-1 I-V CHARACTERISTICS OF A TYPICAL SOLAR CELL.

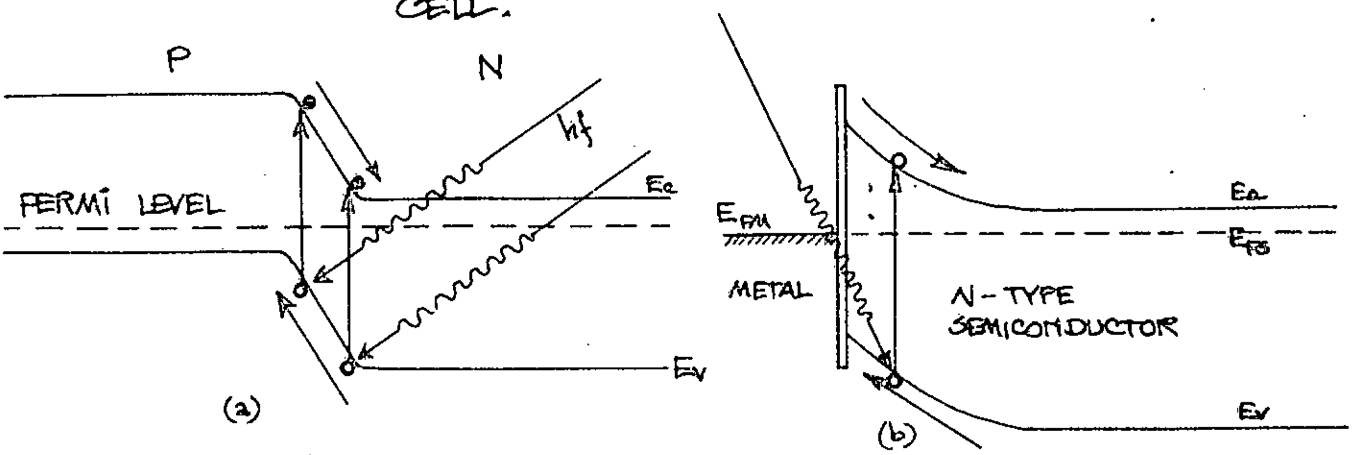

FIGURE 2-2 ENERGY BAND DIAGRAM OF A (a) P-N JUNCTION AND (b) METAL-SEMICONDUCTOR JUNCTION

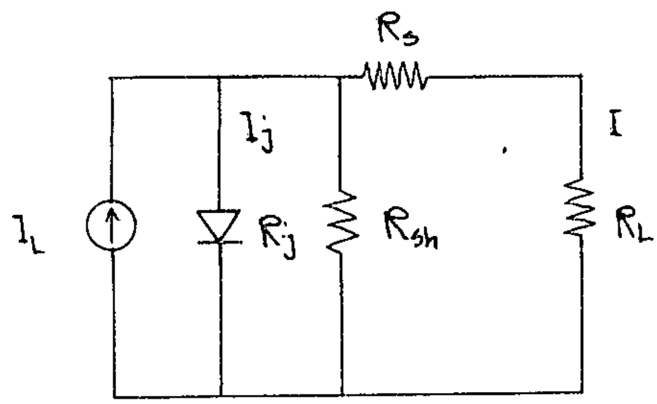

FIGURE 2-3 EQUIVALENT CIRCUIT OF AN ILLUMINATED SOLAR CELL.

have some variations to these basic features.

Because of the barrier layer which is essential for photovoltaic effect, solar cells have diode characteristics in dark. The I-V characteristics of a typical solar cell is shown in Fig. 2.1. A illuminated solar cell connected to a load develops a photocurrent, and a photovoltage in the forward biased mode. Under light, the I-V curve keeps nearly the same shape but shifts along the negative current axis. As a result, an open circuit voltage appears on the positive voltage axis and a short circuit current on the negative current axis. The diode current normally present at this forward bias voltage opposes the photocurrent generated by the light and the maximum power from the solar cell can be obtained by optimizing the product of I and V.

Two rectangles are marked around the I-V characteristics. The ratio of the smaller to the larger rectangle is called the fillfactor. The short circuit current I_{sc}, the open circuit voltage V_{oc} and the 'squareness' of the I-V characteristics (fillfactor) under illumination are often cited as figure of merit of a solar cell although the overriding figure of merit, of course, is the efficiency.

2.3 A REVIEW OF RADIATION PRINCIPLES

In the early years of the present century Max Plank suggested that electromagnetic radiation is emitted discontinuously as little burst of energy which are called quanta. Light, being electromagnetic energy, its quanta is known as photon. Plank found that the quanta associated with a particular frequency f of light all have the same energy and this energy E_p is directly proportional to f. That is

$$E_p = hf \qquad 2.3.1$$

Solar radiation is the energy source which is utilized in photovoltaic devices. The spectral distribution of sunlight depends on many factors, including the three sources of atmospheric absorption,[68] namely

(a) atmosphetic gases (O_2, N_2 and so on)

(b) water vapour

(c) dust.

In each of the absorption processes the ultravoilet is deplected in a preferential manner. The effect of these absorption sources is described by means of an optical path length m through which the light passes, and by means of the number of centimeters of precipitable water vapour W in the atmosphere. The quantity m is defined by the relation m = 1/Cos z, where z is the angle between the line drawn through the observer and the zenith and the line through the observer and the sun. In the course of the day z varies from 90° to a minimum z_{min} which occurs at noon and which is a function of the season of the year.

The photon flux is a quantity which is very useful in the calculation of solar cell performance. It is defined as the number of photons crossing a unit area perpendicular to the light beam per second.

Table 2 below gives some indication of the variation of solar intensity and photon density N_{ph} (Number/sec. cm^2) for various values of m and w. The total number of solar photons N_{ph} covers a range of energy from zero to a maximum energy found in the solar spectrum.

Table 2 Parameter of the Solar Spectrum as a Function of Absorption Condition [68]

m	w	Comments	Ø w/cm^2	Average photon energy E_{av} (ev)	N_{ph} (No./Sec. cm^2)
0	0	Outside atmostphere (Air mass 0)	0.135	1.48	5.8×10^{17}
1	0	Sea level, sun at zenith(Air mass 1)	0.106	1.32	5.0×10^{17}
2	0	Sea level, sun at 60^o from zenith	0.088	1.28	4.3×10^{17}
3	0	Sea level, sun at 70.5^o from zenith	0.075	1.21	3.9×10^{17}
1	2	About 50% relative humidity	0.103	1.21	4.8×10^{17}
3	5	Extreme condition	0.059	1.18	3.2×10^{17}

2.4 THE P-N JUNCTION AND METAL-SEMICONDUCTOR JUNCTION AS A PHOTOVOLTAIC CONVERTER

Fig. 2.2 is an energy band diagram of a p-n junction and MS junction under the action of light. When the junctions are illuminated with light having sufficient energy to excite an electron from the valence band to conduction band a hole is created in the valance band. In the junction there is an built-in electric field and the resulting electron-hole pair move in the directions shown in the diagram. These charges act to charge p-type (or metal for MS junction) region positively and the n-type region negatively. Thus if there is no external connections to the junction, the resulting forward bias causes a forward current to flow. Under these condition the forward current is just equal to the optically generated current. When the p (or metal for MS junction) and n-type sides are connected through an external load, a pat of the generated current flows in it, so that the junction acts as a converter of light energy. In this conversion there no intermediate step of conversion to heat and the Carnot cycle limitation on efficiency of conversion is bypassed. For this reason photvoltaic conversion has shown a great promise to those who have worked in direct energy conversion.

From the above discussion a simplified equivalent circuit Fig. 2.3 of an illuminated photovoltaic cell or solar cell can be drawn. With the help of this simplified but realistic model the operation of the solar cells, which involve microscopic action, can be described in terms of a macroscopic device that yields an equivalent result. The equivalent circuit consists of a constant-current generator delivering a current I_L into a network, which include the nonlinear impedance of the junction R_j, and intrinsic series resistance R_s, an intrinsic shunt resistance R_{sh} and the load resistance R_L. This equivalent circuit diagram is adequate for technological and physical applications of all types of solar cells. The difference lies mainly in the properties of the junction.

2.5 SOLAR CELL CALCULATION

The current-voltage (I-V) characteristics of a solar cell can be expressed as

$$I = I_L - I_o \left[\exp(qV/KT) - 1 \right] \qquad 2.5.1$$

where V is the voltage across the junction. Here the value of R_s is assumed to be negligible and R_{sh} is assumed to have a large value. Under open circuit condition (I=0) the voltage across the cell would be

$$V_{oc} = \frac{KT}{q} \ln \left[\frac{I_L}{I_o} - 1 \right] \qquad 2.5.2$$

The power output of the device would be

$$P = IV = \left[I_L - I_o \left\{ \exp\left(\frac{qV}{KT} \right) - 1 \right\} \right] V \qquad 2.5.3$$

Taking derivative of this equation with respect to V and setting the result equal to zero yields an implicit equation for the voltage that maximizes power.

$$\exp\left[qV_{mp}/(KT)\right]\left[1+qV_{mp}/(KT)\right] = 1 + \frac{I_L}{I_o}$$

$$= \exp\left[qV_{oc}/(KT)\right] \qquad 2.5.4$$

From equations 2.5.1 and 2.5.4 we obtain the current that maximized the power.

$$I_{mp} = \frac{\left[qV_{mp}/(KT)\right] I_L}{1 + qV_{mp}/(KT)} \left[1 + \frac{I_o}{I_L}\right] \qquad 2.5.5$$

The maximum power is then given by

$$P_{max} = I_{mp}\ V_{mp} \qquad 2.5.6$$

But since $I_L >> I_o$

$$P_{max} \cong \frac{\left[qV^2_{mp}/(KT)\right] I_L}{1+qV_{mp}/(KT)} \qquad 2.5.7$$

The efficiency of the solar cell is obtained if the solar power density P_{in} is known. Thus the maximum efficiency of the solar cell is given by

$$\eta_{max} \cong \frac{\left[qV^2_{mp}/(KT)\right] I_L}{1 + qV_{mp}/(KT)} \ (P_{in}A)^{-1} \qquad 2.5.8$$

where A is the solar cell area.

2.6 THEORETICAL CONSIDERATIONS

Theoretical power output and efficiency can be easily calculated based on AM1 sunlight of 103 mW/cm^2(39). Maximum current generation is calculated from

$$J_m = q\ \emptyset_1 f \qquad 2.6.1$$

For AM1 sunlight only 2.6×10^{17} photons/sec.cm^2 have energies in excess of the silicon energy gap, E_g = 1.1 ev. This produces a maximum current density J_m = 41.6 mA/cm^2. An open circuit voltage of 0.6 volts, I-V curve fillfactor FF = 0.7, transmittance T = 0.9 produces a power output P_o = 15.7 mW/cm^2 for an efficiency of 15.7%. This simplified calculation has neglected recombination and series resistance losses and involves the formula

$$FF = \frac{J_{mp} V_{mp}}{J_{sc} V_{oc}} \qquad 2.6.2$$

$$J_{sc} = T_c' J_m \qquad 2.6.3$$

$$P = FF\, J_{sc} V_{oc} \qquad 2.6.4$$

This calculation shows that a 15% efficiency should be realized using a Schottky structure for solar energy conversion. This efficiency depends on maximizing solar energy transmission into the device.

2.7 SERIES RESISTANCE

Like any energy source, internal resistance is a parasitic, power consuming factor in diodes and solar cells that can degrade the device performance. Because of this series resistance, the maximum available power output is decreased and this is reflected in the current voltage characteristics. It has been shown[62] that in normal sunlight conditions, about 10-20% of the originally available power is lost just from an additional increase of one ohm of resistance. In fact, series resistance is one of the key parameters in solar cell fabrication technology.

It has been found that to improve the collection efficiency the active layer on the top of the junction has to be reduced in thickness because of the larger photon absorption. But this causes an inevitable rise in resistance values. The older deeper diffused cell resistances were, limited by contact resistances. The present day solar cells with current collecting grid lines on the top, however, are usually limited by the resistance in the active sheet region due to the very small cross-sectional area which the carriers in this region traverse, while the contact resistance has been made negligible, for the most part, by the technology of the contact fabrication. This has been discussed in some detail in section 4.2.2.

The series resistance of a Schottky barrier solar cell is mainly due to metal-semiconductor contacts at the back, bulk semiconductor resistance, transverse sheet resistance of the barrier metal, and the resistance of the grid structure.

The conducting grids on the active surface of the present day solar cell reduces the average path length of a carrier in the active region which greatly minimizes the resistance of the active region. Since, however, the area under the grid itself contributes nothing to current generation due to the fact that all the usable light is absorbed by the metal current collecting grid lines, there is an upper limit to the number and size of the grids which can be deposited for optimum performance of the solar cell in any given environment and for a given values of the solar cell parameter except the antireflection coating. By using the detailed analysis of series resistance developed by Handy[57], the loss due to resistance can be included in the I-V relationship and the equivalent diagram of the solar cell.

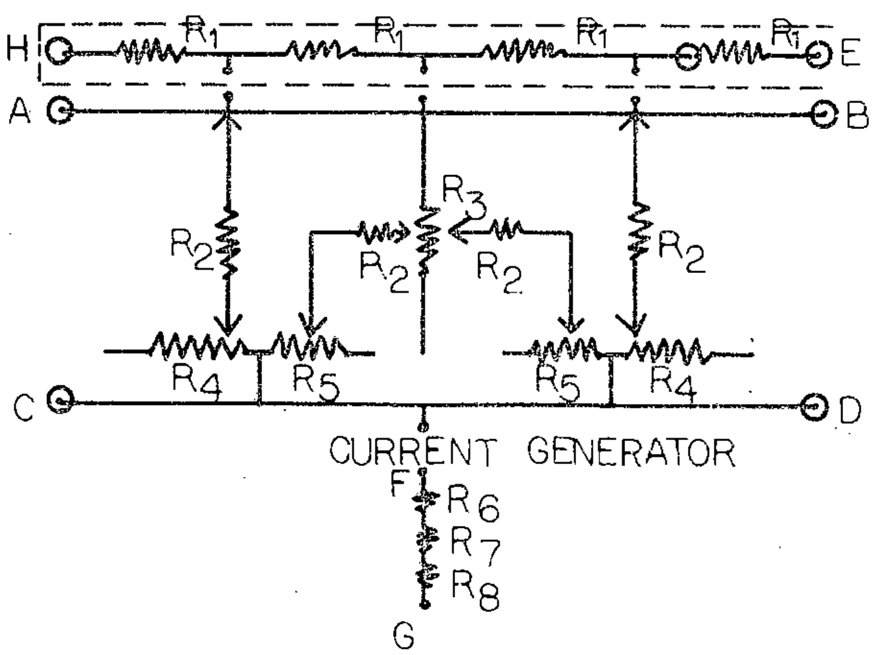

R_1 = RESISTANCE OF CONTACT STRIP

R_2 = CONTACT RESISTANCE BETWEEN ACTIVE REGION AND ELECTRODES

R_3 = RESISTANCE OF GRID STRIP

R_4 = RESISTANCE OF THE ACTIVE REGION FOR CARRIERS FLOWING TO CONTACT STRIP

R_5 = RESISTANCE OF THE ACTIVE REGION FOR CARRIERS FLOWING TO GRID STRIP

R_6 = RESISTANCE OF BULK REGION

R_7 = CONTACT RESISTANCE OF THE BULK REGION TO BOTTOM ELECTRODE

R_8 = RESISTANCE OF BOTTOM ELECTRODE

FIGURE 2.4 EQUIVALENT RESISTANCE OF SOLAR CELL (

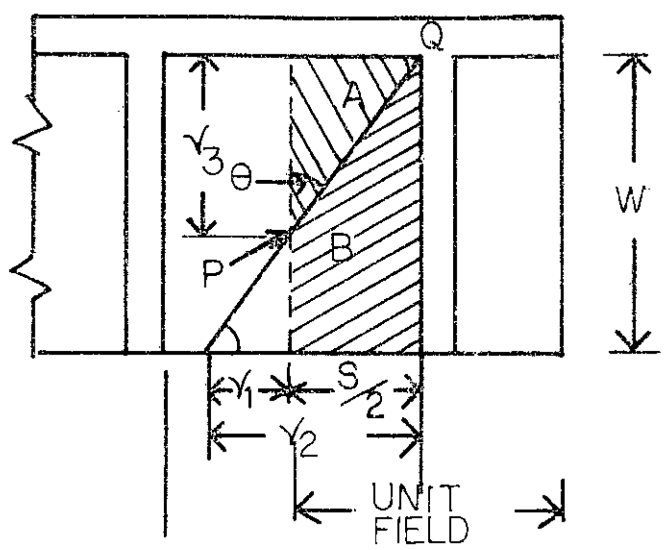

FIGURE 2.5
UNIT FIELD DEVIDED INTO TWO PARTS

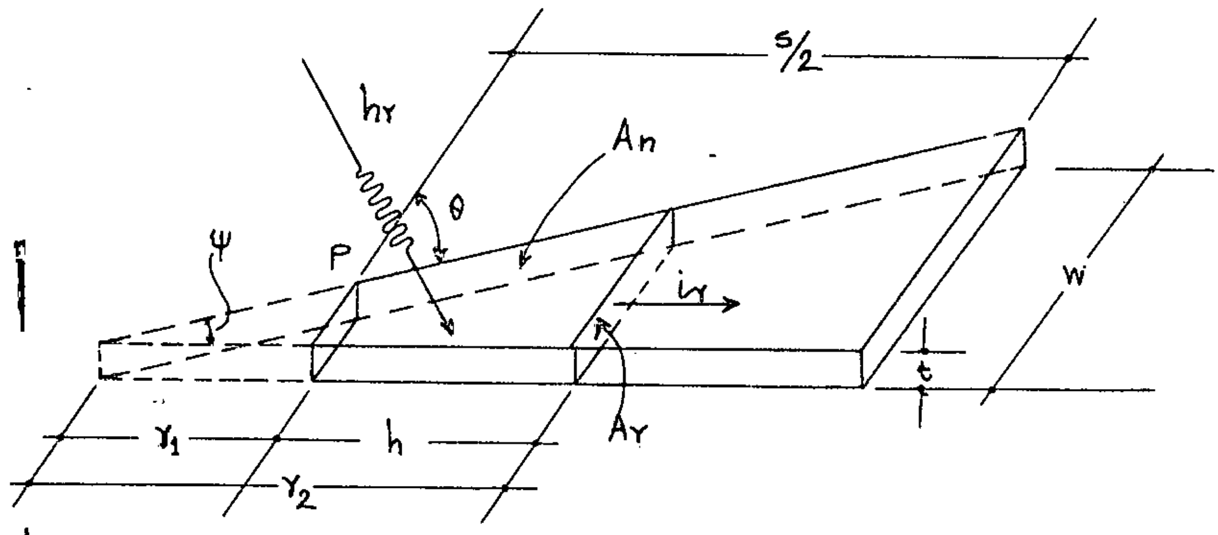

FIGURE 2.6. TRAPEZOIDAL REGION OF UNIT-FIELD REPRESENTING R_5

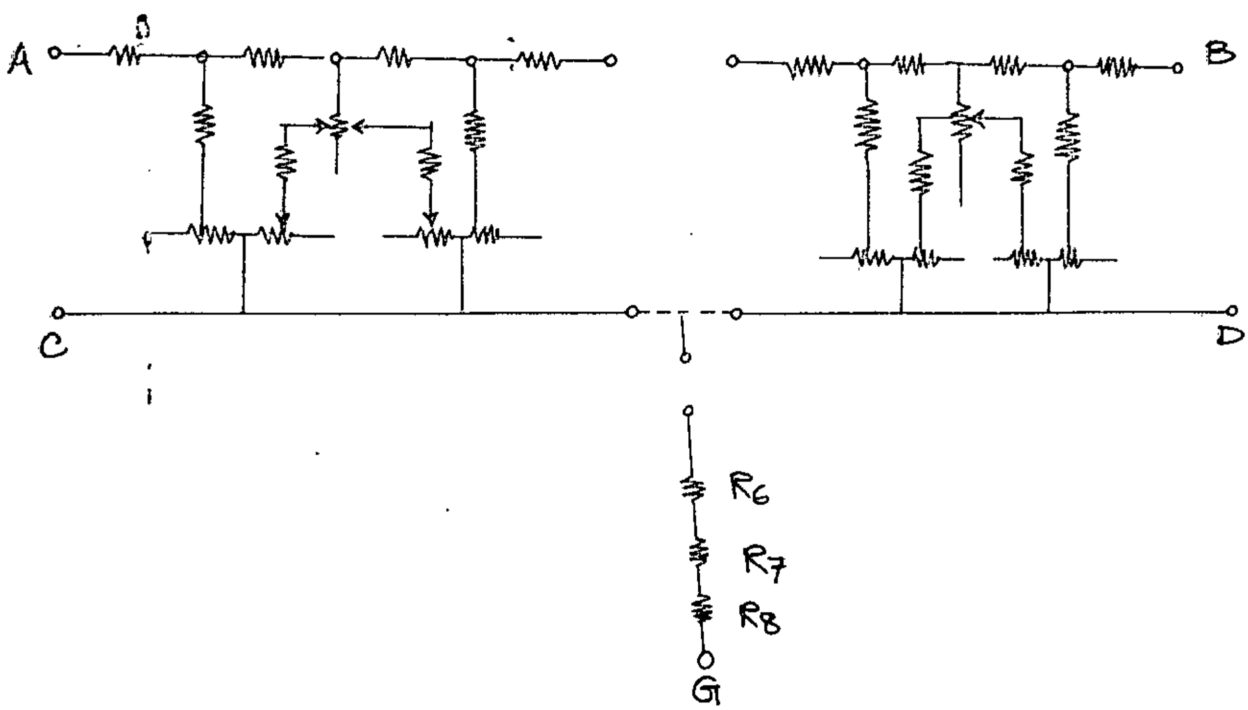

FIGURE 2-7.
REPRESENTATION OF A N-UNIT FIELD SOLAR CELL.

The equivalent resistance circuit of the solar cell is shown in Fig. 2.4. The series resistance of the solar cell are of two distinct types, namely:

(1) resistance of the active region which is a distributed resistance determined by a nonuniform current distribution, and

(2) other resistance which can be lumped' as they are uniformly traversed by the current passing through the cell.

Resistances R_4 and R_5 fall in the first category. Determination of these resistances presents a different problem than the other resistances in the equivalent circuit, since these resistances are not physically separable for individual measurement because of the fact that current density in this region is not uniform as current generation occurs over the entire region. The active region of the solar cell can be broken up into identical parts which corresponds to a unit field Fig. 2.5. Within one unit field there are two areas which are symmetrical about the grid line and have dimensions $\frac{1}{2}S\times W$. The resistance contributed by the regions A and B are R_4 and R_5 respectively.

The line CD is an artificial boundary which seperates the two region from which the current flows to the contact strip and from which current flows to the grid strip. The trapezoidal region representing resistance R_5 is shown in Fig. 2.6. The total current flowing towards the grid strip through the area A_r is given by

$$i_r = (J_r)(r_2 \tan\psi)t \qquad 2.7.1$$

where

t = thickness of media

$r_2 \tan\psi$ = length of the rectangular area A_r

J_r = current density through A_r

From continuity equation

$$i_n = i_r \qquad 2.7.2$$

where i_n = current produced by photon absorption in the area A_n. If J_n is the generated current density in the normal direction to A_n, it can be written in the following form.

$$J_n A_n = J_r t(r_2 \tan\psi) \qquad 2.7.3$$

From Fig. 2.6 we have

$$A_n = \tfrac{1}{2}h\,(r_1 + r_2) \tan\psi \qquad 2.7.4$$

and since $h = r_2 - r_1$, we have

$$J_r = \frac{J_n(r_2^2 - r_1^2)}{2r_2 t} \qquad 2.7.5$$

using the above relations. Putting equation 2.7.5 into 2.7.1 one obtains

$$i_r = \tfrac{1}{2}\left[J_n(r_2^2 - r_1^2)\tan\psi\right] \qquad 2.7.6$$

For one-dimensional linear homogeneous current flow we have

$$E_r = J_r\rho \qquad 2.7.7$$

where E_r = Electric field

ρ' = resistivity of metal

Putting equation 2.7.5 in 2.7.7 we have

$$E_r = \frac{J_n(r_2^2 - r_1^2)\rho'}{2r_2 t} \qquad 2.7.8$$

The potential that is produced by an electric field may be calculated from

$$\varnothing = \int_{path} E.dr \qquad 2.7.9$$

where dr represents the path over which the field exists. Thus we can calculate the potential that will exist in the media due to the field produced by light generated charges.

The potential is given by

$$\varnothing = \int_{r_1}^{r_2} \frac{J_n(r_2^2 - r_1^2)\rho'}{2r_2 t} dr_2 \qquad 2.7.10$$

In the determination of the resistance R_5, r_1 is constant, r_2 is the variable of integration. Thus it can be written in the following form:

$$\varnothing_{R_5} = \frac{\rho' J_n}{2t} \left\{ \int_{r_1}^{r_2} r dr - r_1^2 \int_{r_1}^{r_2} \frac{dr}{r} \right\} \qquad 2.7.11$$

Similarly we have

$$\varnothing_{R_4} = \frac{\rho' J_n}{2t} \int_0^{r_3} r dr \qquad 2.7.12$$

where $r_1 = \frac{S(W - r_3)}{2r_3}$ and $r_2 = \frac{SW}{2r_3}$

Assuming ϕ_{R_4} and ϕ_{R_5} equal at point P and guranteeing that there is no current flow across the line CD we have

$$\left(\frac{2r_3}{S}\right)^2 = \frac{2W}{r_3} - 1 - 2\left(\frac{W}{r_3} - 1\right)^2 \ln\left(\frac{W}{W-r_3}\right) \qquad 2.7.13$$

The solution of the above equation gives the value of r_3 for a given configuration.

The total current flowing through R_5 is given by

$$i_r = J_n \tfrac{1}{4} S(2W-r_3) \qquad 2.7.14$$

From Ohm's law, the value of R_5 is given as

$$R_5 = \frac{2\rho'}{St(2W-r_3)} \operatorname{Sin} \theta_i \left\{ \int_{\frac{S(W-r_3)}{2r_3}}^{SW/2r_3} r\,dr - \frac{S^2(W-r_3)^2}{4r_3^2} \int_{\frac{S(W-r_3)}{2r_3}}^{SW/2r_3} \frac{dr}{r} \right\} \qquad 2.7.15$$

Similarly

$$R_4 = \frac{2\rho'}{Str_3} \operatorname{Cos} \theta_i \int_0^{r_3} r\,dr \qquad 2.7.16$$

The $\sin \theta_i$ and $\operatorname{Cos} \theta_i$ terms are introduced to recognise the fact that the electric field E_r not in the direction of the path.

Fig. 2.7 shows the representation of a n-unit field solar cell. The total series resistance R_T between points A and G can be represented by the following equation.

$$R_T = \frac{R_C}{1+(R_C/R_P)} + R_1 + R_6 + R_7 + R_8 \qquad 2.7.17$$

where

$$R_C = \frac{\left\{1 + \frac{R_1}{R_3 + \frac{1}{2}(R_2 + R_5)} + \frac{R_1}{R_1 + R_2 + R_4}\right\}(R_2+R_4)}{2 + \frac{R_1 + R_2 + R_4}{R_3 + \frac{1}{2}(R_2+R_5)}} \qquad 2.7.18$$

and

$$R_p = \frac{2R_C\ (R_C + R_1)}{(n-1)(2R_C + R_1)} \qquad 2.4.19$$

2.8 OPTIMIZING GRID SPACING

For low series resistances the I-V characteristics of the solar cell can be expressed as

$$I = I_o \left[\exp(\frac{qV}{nKT}) - 1 \right] - I_L \qquad 2.8.1$$

But for high values of series resistance the effect of the resistance must be considered and the following equation is applicable.

$$I = I_o \left[\exp\left\{ \frac{q}{nKT} (V - IR_s) - 1 \right\} \right] - I_L \qquad 2.8.2$$

By utilizing equation 2.7.17 it is possible to optimize the grid specing to obtain the most advantageous configuration. But unfortunately it is not only enough to simply minimize R_T as this would result in a cell which had 100 percent of its surface covered by grid contacts. An optimum between minimum resistance and maximum current generation must be calculated. A computer program has been developed which obtains R_T as a function of grid specing and finds the optimum value of grid spacing for the maximum value of short circuit current of a solar cell of a given dimension. The dimension of the cell was

1.5 cm x 0.9 cm, resistivity of metal $\rho_o' = 200\ \mu\Omega$-cm, the generated current density $J_m = 40$ mA/cm^2, dark saturation current I_o for cell was assumed to be 1×10^{-6} ampere. It was assumed that all other resistance contributions are zero and the only contribution to resistance is from the active sheet resistance. The width of the grid was (1) .0025 cm and (2) 0.5 cm respectively. The cell was then subdivided into several unit-fields and the corresponding short circuit current and internal series resistances are calculated. The theory of resistance calculation has been discussed in section 2.7. The results obtained are shown graphically in Fig. 2.8. Subscript (1) and (2) denotes the two cases. It is clearly shown in the figure that if the grid line width is large, with the increase in number of grid lines the short circuit current value decreases very fast.

If the grid lines width is very narrow, the decrease in current is negligible. As a consequence if small value of series resistance is desired, the unit field width can be decreased widthout appreciable loss of short circuit current. But in the second case if maximum short circuit current is desired, the resistance will have high value and as a consequence the fill factor will deteriorate.

```
      OPTIMIZATION OF GRID STRUCTURE OF SOLAR CELLS.
      W=WIDTH OF SOLAR CELL, T=WIDTH OF GRID STRUCTURE,RO=RESISTIVITY.
      TL=TOTAL LENGTH OF CELL,JM=MAXIMUM CURRENT DENSITY,
      DM=MINIMUM LENGTH WHICH CAN BE ACHIEVED.
      REAL JM,IO
      WRITE(3,888)
  888 FORMAT('1',42X,'OPTIMIZATION OF GRID STRUCTURE OF SOLAR CELLS')
      READ(1,1) W,T,TL,DM,RO,JM,G,IO,THICK
    1 FORMAT(7F8.4,2E10.3)
      B=1./(Q*26.)
      SD=.01
      N=1
   76 ALC=TL/FLOAT(N)
      S=ALC-T
      IF(S.LT.0.05) GO TO 77
      AN=N
      WRITE(3,100) S
  100 FORMAT(///55X,'SEPARATION OF GRIDS=',F14.7,' CM')
      NO=W/SD
      DO 3 J=1,NO
      RR3=SD*FLOAT(J)
      X=(2.*RR3/S)**2-(2.*W/RR3-1)+2.*((W/RR3-1)**2)*ALOG(W/(W-RR3))
      IF(J.EQ.1) GO TO 6
      IF(ABS(X).GT.ABS(X1)) GO TO 3
      X1=X
      R3=RR3
      GO TO 3
    6 X1=X
      R3=RR3
    3 CONTINUE
      WRITE(3,10) R3,X1
   10 FORMAT(36X,'R3=',E14.7,15X,'DIFFERENCE =',E14.7)
      TH=ATAN(S/(2.*R3))
      RX=2.*RO/(S*THICK*(2.*W-R3))
      R4=RO*R3*(COS(TH))/(S*THICK)
      D=(S*W/(2.*R3))**2
      E=(S*(W-R3)/(2.*R3))**2
      THD=TH*57.29578
      R5=RX*(SIN(TH))*((D-E)/2.-E*ALOG(W/(W-R3)))
      RT1=R4*R5/(R4+R5)
      WRITE(3,11) THD,R4,R5,ALC,N
   11 FORMAT(/9X,'THETA=',F8.4,'DEGREE',9X,'R4=',F10.5,9X,'R5=',F10.5,9X
     1,'UNIT LENGTH=',F10.6,9X,'NO. OF UNITS=',I4/)
   90 AREA=W*TL
      RT=RT1/(2.*AN)
      AEFF=AREA-AN*W*
      WRITE(3,14) RT, EFF,AREA
   14 FORMAT(/4X,'TOTAL SERIES RESISTANCE RT=',E14.7,' OHM',4X,'EFFECTIV
     1E AREA AEFF=',E14.5,4X,'ACTUAL AREA=',E14.5)
      AL=JM*AEFF
      AISC=.0
      YY=.0
      MM=  /.0625+1.
      DO 5  I=1,MM
```

```
      G=II-1
      AI=.0625*G
      POW=B*AI*RT
      IF(POW.GT.173.) GO TO 5
      Y=AI-AL+IO*(EXP(POW)-1.)
      IF(II.EQ.1) GO TO 8
      IF(ABS(Y).GT.ABS(YY)) GO TO 5
    8 YY=Y
      AISC=AI
    5 CONTINUE
      WRITE(3,15) AISC,YY
   15 FORMAT(/25X,'SHORT CIRCUIT CURRENT ISC=',E14.5,20X,'ACCURACY='
     1,E14.8)
    2 CONTINUE
      N=N+1
      GO TO 76
   77 WRITE(3,16)
   16 FORMAT(//60X,'END OF JOB')
      CALL EXIT
      END
```

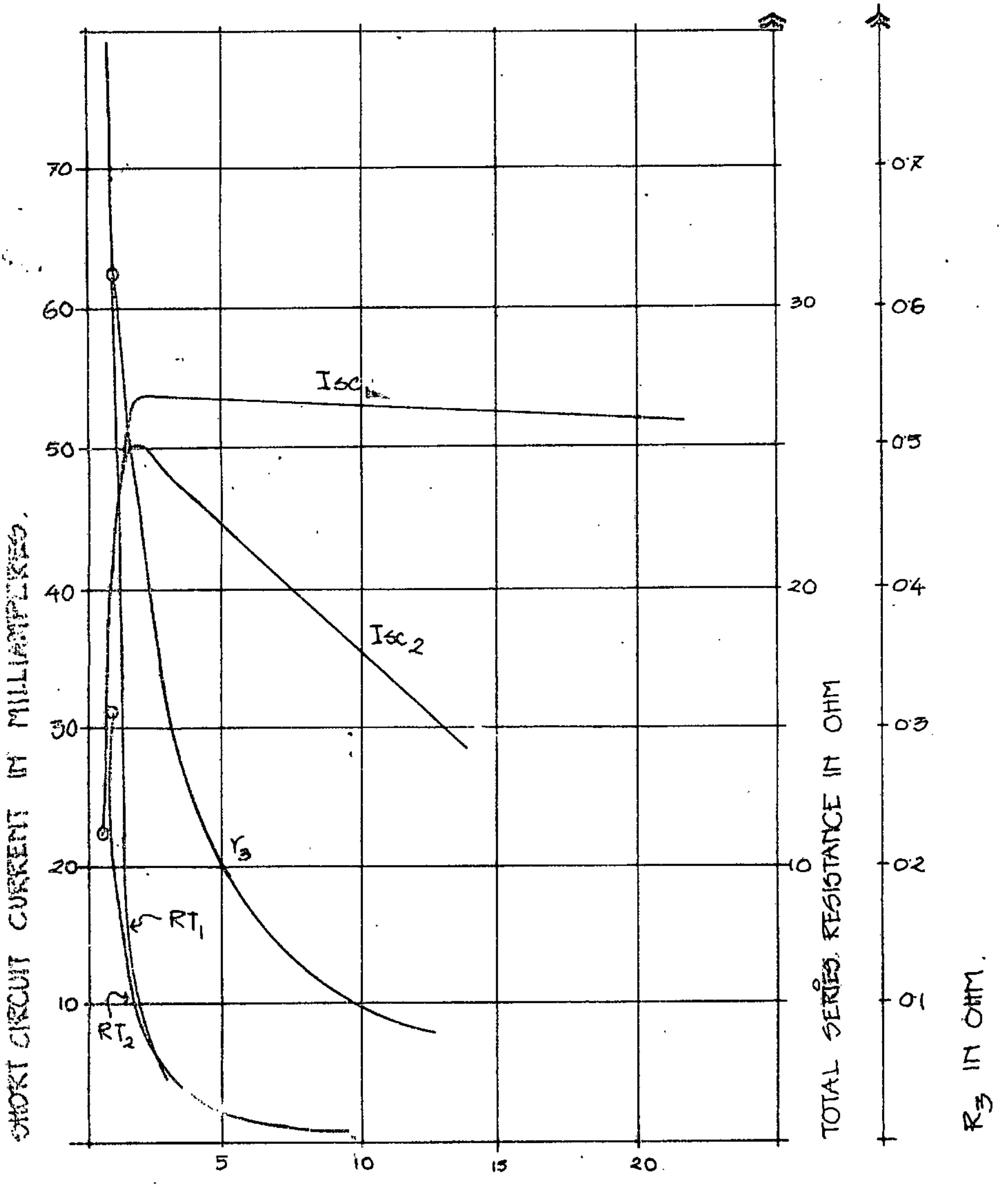

FIGURE _ 2·8
COMPUTER RESULTS FOR GRID OPTIMIZATION.
(FOR TWO VALUES OF WIDTH OF GRID LINES.)

CHAPTER III

THEORY OF SCHOTTKY BARRIER AND MIS SOLAR CELLS

3.1 PRELIMINARIES

In this chapter Schottky barrier and Metal-Insulator-Semiconductor (MIS) solar cells have been discussed in details. A theoretical discussion on the interface effects in MIS solar cells has been presented together with the expression of current of the solar cell for illuminated condition. A derivation of expression of forward tunnel current in the presence of an insulating layer has been shown and an expression of tunneling transmission probability has been presented. It has also been shown in these derivations that the oxide interfacial layer results in an enhancement of open circuit voltage V_{oc} which is one of the major factors in obtaining higher conversion efficiency.

3.2 SCHOTTKY BARRIER SOLAR CELLS

Solar cells utilizing homojunctions in Si and hetrojunction with GaAs and CdS have already demonstrated the effectiveness of photovoltaics in generating electricity on earth. However, if photovoltaics is to emerge as a method capable of providing large-scale electric power, then a cost of reduction of around 50 times or more must be achieved in the solar cells (or solar cells plus concentrators in concentrated sunlight systems).

One of the possibilities for cost reduction lies in the method of junction fabrication and the idea of a simple deposited Metal-Semiconductor (MS) junction is, at the first sight very attractive. Metal deposition method are consistent with high yield, fast processing, and also involve low temperature. The MS solar cell would appear to be very promising on account of the simplicity of fabrication and the fact that with a suitable antireflection coating and barrier metal thickness, highly efficient coupling of ambient photon energy to the metal-semiconductor interface is possible. Also, in these cells, the semiconductor depletion layer begins at this latter interface and thus, when compared to the bulk junction devices, increased short-wave length response should result.

Thus these metal-semiconductor solar cells offer a possible solution for future applications. Reduced silicon processing costs present a method for economical energy conversion. Schottky barrier diodes can be formed by simply depositing an ohmic metal, heat treatment (HT) to form ohmic contact, depositing a semitransparent barrier metal, and applying contacts. This could all be accomplished with one pump-down of proper vacuum system. Schottky barrier solar cells (SBSC) offer design flexibility in choice of alloy and pure metals, metal thickness, and antireflection coatings. SBSC theory developed from work on single crystal silicon can be extended to work on polycrystalline silicon for future large area SBSC.

3.3 MIS SOLAR CELLS

In practice, however, intimate contact metal-semi-conductor solar cells exhibit a serious deficiency in the form of very poor photovoltaic response. This stems from the fact that the usual thermionic dark current in Schottky barrier junction leads to a considerably higher dark current than many homojunction and heterojunction structures. Theoretical and practical work indicated that it is possible to overcome this disadvantage, yet still preserve the attractive Schottky barrier technology, by allowing a very thin insulating layer to separate the metal and semiconductor. The deliberate introduction of such a layer yields a Metal-Insulator-Semiconductor (MIS) solar cells and hence can not be classed as ideal Schottky barrier. The principle beneficial effect of the thin insulating layer is the increasing of the photovoltage, brought about by either (or both) control of the current transport through the diode or an increase in diode ideality factor n. As increases in n (particularly $n > 2$) can be detrimental to the fill factor, control of diode current transport properties becomes importance. In MIS structure the thermionic emission dark current can be reduced by either increasing the effective metal-semiconductor barrier height, decreasing the probability of majority carrier tunneling, encouraging interface states with large capture cross-section for majority carriers, or reducing the number of majority carriers at the semiconductor surface.

3.4 INTERFACE EFFECTS IN MIS SOLAR CELLS

It is well known that when a metal contact is evaporated onto a chemically prepared silicon surface the metal and semiconductor are not in intimate contact. An interfacial film of of atomic dimentions inevitably separates the two. This metal-

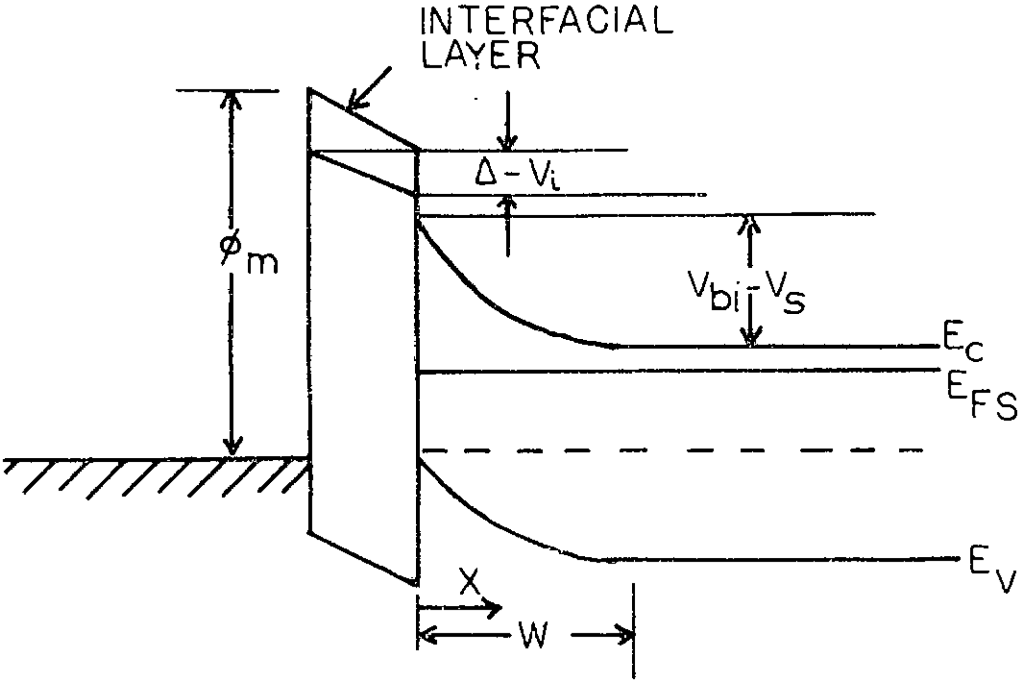

JRE 3.1 ENERGY BAND DIAGRAM FOR ANTIREFLECTION COATED-MIS CELL UNDER ILLUMINATION

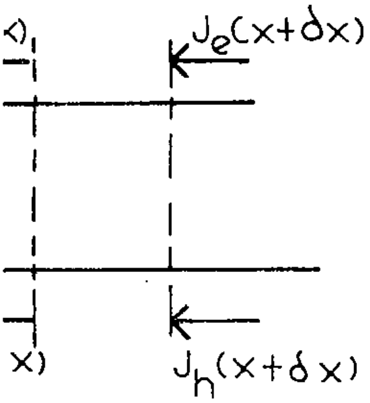

RE 3.2
RAM ILLUSTRATING
RGE CONSERVATION

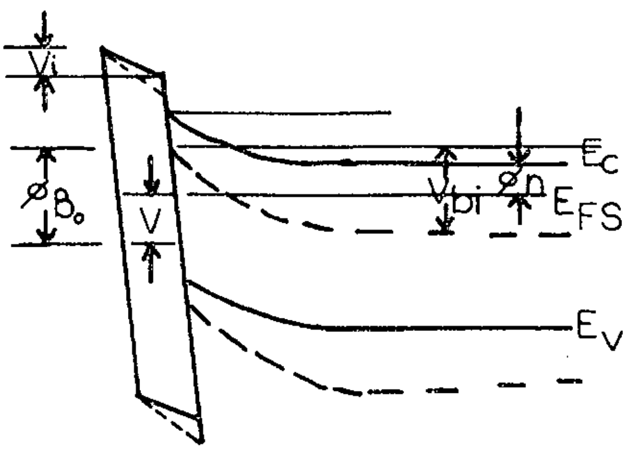

FIGURE 3.3
ENERGY BAND DIAGRAM OF THE CHEMICALLY PREPARED MIS CONTACT (AT ZERO BIAS —— UNDER AN APPLIED (FORWARD) BIAS)

insulator-semiconductor (MIS) or metal-oxide-semiconductor (MOS) diode is the most useful device in the study of semiconductor surfaces. Since the reliability and stability of all semiconductor devices are intimately related to their surface conditions, and understanding of surface physics with the help of MIS diodes is of great importance to device operations.

The energy band diagram for antireflection-coated metal-oxide-semiconductor (AMOS) solar cells is given in Fig. 3.1 for illuminated conditions. It may be seen that when the device is developing a voltage V, V_s is developed across the semiconductor and V_i is developed across the interfacial oxide layer so that[27]

$$V = V_i + V_s$$

At this voltage, we now seek to find the contribution to the total current due to light induced photocurrent and recombination current within the transition region. By conservation of charge Fig. 3.2 and taking the current density as positive when it is flowing to the left i.e in the reverse direction, the net recombination rate is (U-F).

The number of excess electrons lost due to recombination rate in element ∂x is given by

$$(U-F)\partial x = \frac{1}{-q}\left[J_e(x+\partial x) - J_e(x)\right]$$

$$= -\frac{1}{q}\frac{dJ_e(x)}{dx}\partial x \qquad 3.4.1$$

$$\text{or } q(U-F) = -\frac{d\,J_e(x)}{dx} \qquad 3.4.2$$

Similarly for hole current density $J_h(x)$,

$$q(U-F) = + \frac{d\, J_h(x)}{dx} \qquad 3.4.3$$

These equationsgive

$$J = J_e(x) + J_h(x) \qquad 3.4.4$$

The total current density J flowing through the junction under illuminated condition is given by

$$J = J_e(0) + J_h(0) \qquad 3.4.5$$

$$= J_e(0) + J_h(W) - q \int_0^W (U-F)\, dx \qquad 3.4.6$$

If Schottky barrier lowering effects are neglected and if the transmission probability for electrons tunneling through the interfacial layer is assumed to be unity, it follows that

$$J_{ms}^{e} = A^{*}\, T^2\, e^{-q\phi_B/KT}\, e^{-qV_i/KT} \qquad 3.4.7$$

and

$$J_{sm}^{e} = A^{*} T^2\, e^{-q\phi_B/KT}\, e^{qV_s/KT} \qquad 3.4.8$$

Thus $J_e(0)$ is given by

$$J_e(0) = J_{ms}^{e} - J_{sm}^{e} \qquad 3.4.9$$

The current density $J_h(W)$ is found from

$$J_h(W) = qD_p \left. \frac{dp(x)}{dx} \right|_{x=W} \qquad 3.4.10$$

where p(x) is the hole concentration in semiconductor valence band which satisfies the equation[63]

$$\frac{d^2p}{dx^2} - \frac{p-p_{no}}{D_p \tau_p} + \frac{F(x)}{D_p} = 0 \qquad 3.4.11$$

$$\text{where} \quad F(x) \equiv \int_{\lambda_0}^{\lambda_1} \alpha \Phi e^{-\alpha x} d\lambda \quad sec^{-1} \; m^{-2} \quad (64) \qquad 3.4.12$$

where λ_0, λ_1 = hc/qE_g indicate the wave length limits for the incident solar spectrum. The generation rate F has been modelled as shown with Φ as the photon flux incident to the semiconductor and α as the absorption coefficient as a function of wavelength.

The boundary conditions are (1) $p(x) \rightarrow p_{no}$, the unilluminated hole concentration far from the junction as $x \rightarrow \infty$. (2) $p(W) = p^* + p_{no}$; where p^* is given by the expression

$$p^* = p_{no} \left\{ \exp(q/KT) \left[E_{Fs} - E_{Fp}(W) \right] -1 \right\} \qquad 3.4.13$$

The value of Fermi level $E_{Fp}(W)$ depends on the details of processes occuring at this boundary including hole transport across the interfacial layer. In the case of excellent communication between the metal and valence band of semiconductor $E_{Fp}(W) \approx E_{Fp}(0) = E_{Fm}$. With the above assumptions of a flat quasi-Fermi level through the depletion region, p^* in this case is given by

$$p^* = p_{no} \left[\exp(qV/KT) -1 \right] \qquad 3.4.14$$

Consequently it is found that

$$J_h(W) = \int_{\lambda_0}^{\lambda_1} \frac{q\alpha \Phi L_p \, e^{-\alpha W}}{1 + L_p \alpha} d\lambda - \frac{qp_{no}}{L_p} D_p (e^{qV/KT} -1) \qquad 3.4.15$$

The contribution of current density from the depletion region is given by

$$J_T^D = q\int_0^W (F-U)\,dx \qquad 3.4.16$$

$$= q\int_0^W \int_{\lambda_0}^{\lambda_1} \alpha \bar{\Phi} e^{-\alpha x}\, d\lambda\, dx - q\int_0^W U dx$$

$$= \int_{\lambda_0}^{\lambda_1} q\bar{\Phi}(1 - e^{-\alpha W})\, d\lambda - q\int_0^W U dx$$

$$= J_{DL}^{\ e} - J_{D_{rec}} \qquad 3.4.17$$

Again

$$J_{D_{rec}} = J_{D_{ifr}} + J_{D_{unav}} \qquad 3.4.18$$

Thus the current density flowing through the device is given by

$$J = J_{ms}^{\ e} - J_{sm}^{\ e} + J_h(W) + J_{DL}^{\ e} - J_{D_{ifr}} - J_{D_{unav}} \qquad 3.4.19$$

The total light current is given from equations 3.4.15 and 3.4.17,

$$J_L = \int_{\lambda_0}^{\lambda_1} \left\{ \frac{q\alpha\bar{\Phi} L_p\ e^{-\alpha W}}{1 + L_p\ \alpha} + q\bar{\Phi}(1 - e^{-\alpha W}) \right\} d\lambda$$

$$= \int_{\lambda_0}^{\lambda_1} \left\{ q\bar{\Phi} - \frac{q\ \bar{\Phi}\ e^{-\alpha W}}{1 + L_p \alpha} \right\} d\lambda \qquad 3.4.20$$

If recombination in the surface region ($0 \leqslant x \leqslant W$) and surface recombination at $x = 0$ are neglected, the total current is given by

$$I = qA\left[\int_{\lambda_0}^{\lambda_1}\left\{\Phi - \frac{\Phi}{1 + L_p\alpha} e^{-\alpha W}\right\} d\lambda\right.$$

$$- A^{*}T^{2}\exp\left(-\frac{q\phi_B}{KT}\right)\left\{\exp\left(\frac{qV_s}{KT}\right) - \exp\left(-\frac{qV_i}{KT}\right)\right\}$$

$$\left. - \frac{p_{no}D_p}{L_p}\left\{\exp\left(\frac{qV}{KT}\right) - 1\right\}\right] \qquad 3.4.21$$

The effects of the interface may be summarized by noting that for a given bias V the largest current will be produced if the interfacial layer is such that the equation 3.4.14 is valid. Further, with an interfacial layer equation 3.4.21 can be written

$$I = qA\left[\int_{\lambda_0}^{\lambda_1}\left\{\Phi - \frac{\Phi\exp(-\alpha W)}{1 + L_p\alpha}\right\} d\lambda\right.$$

$$- A^{*}T^{2}\exp\left(-\frac{q\phi_B}{KT}\right)\exp\left(-\frac{qV_i}{KT}\right)\exp\left(\frac{qV}{KT}\right)$$

$$\left. - \frac{p_{no}D_p}{L_p}\left\{\exp\left(\frac{qV}{KT}\right) - 1\right\}\right] \qquad 3.4.22$$

Where the saturation current is neglected in comparison with other terms. For this interfacial layer V_i has the range(44)

$$\frac{C}{(1+qD_{ss}\delta/\epsilon_i)}\left[(V_{bi})^{\frac{1}{2}} - (V_{bi} - V_s)^{\frac{1}{2}}\right] \leq V_i \leq$$

$$\frac{\delta q D_{ss} V_s}{\epsilon_i} + C\left[(V_{bi})^{\frac{1}{2}} - (V_{bi} - V_s)^{\frac{1}{2}}\right] \qquad 3.4.23$$

i.e $V_i \geq 0$ and since equation 3.4.14 is valid if no interfacial layer existed, it is seen that for a voltage V a larger current is produced than would be if there were no interfacial layer. That is, it can be seen that the fill factor has been improved.

It may also be noticed from equation 3.4.22 that the open circuit voltage has been enhanced by the presence of this interfacial layer. An even further advantage could be achieved if the interfacial layer is designed such that it is not as efficient in the transport of conduction band electrons i.e if the tunneling of conduction band electrons through the insulator is entirely negligible equation 2.4.22 reduces to

$$I = qA \left[\int_{\lambda_o}^{\lambda_1} \left\{ \Phi - \frac{\Phi \exp(-\alpha W)}{1 + L_p \alpha} \right\} d\lambda - \frac{p_{no} D_p}{L_p} \left\{ \exp\left(\frac{qV}{KT}\right) - 1 \right\} \right] \qquad 3.4.24$$

Among effects omitted in the above theory we have the following:

(a) The light current has been calculated on the basis employed by Fonash[44]. The holes and electrons are generated in the depletion region and they tend to move to right and left respectively on Fig. 3.1 without recombination giving J_{DL}^{e}. The remaining photons generate carriers in the bulk region and they are subject to recombination (first term of equation 3.4.15). The corresponding result without recombination is obtained if L_p is imagined to become very large. The reduction of light current due to electrons tunneling from the metal has not been included. This causes J_L and J to be overestimated.

(b) Another cause of an overestimation of J arises from an underestimation of J_{sm}^{e} due to the neglect of image force lowering of the potential near x = 0. The effect of image force lowering on J_{ms}^{e} is likely to be rather small.

3.5 THE FORWARD (TUNNEL) CURRENT

Barden has written the probability per unit time of the transition of an electron in a state a on one side of tunneling region to a state b on the otherside.

$$P_{ab} = (2\pi/\hbar)|M_{ab}|^2 \rho_b f_a (1 - f_b) \qquad 3.5.1$$

where M_{ab} is the matrix element for the transition, ρ_b is the density of states at b, and f_a and f_b are the probabilities of occupation of the states a and b, respectively. This is a direct application of the 'golden rule' of time-dependent perturbation theory.

M_{ab} vanishes unless the transverse wave number is the same for the initial and final states (specular transmission); thus ρ_b is a density of states for fixed K_t. We sum over all states a for fixed K_t; sum over K_t, multiply by 2 for spin and multiply by the electron charge q to obtain the total current to the right. Subtracting the current to the left, we finally have[65]

$$J = \frac{4\pi q}{\hbar} \sum_{K_t} \int_{-\infty}^{\infty} |M_{ab}|^2 \rho_a \rho_b (f_a - f_b) dE \qquad 3.5.2$$

It will be assumed throughout that K_t is conserved in each transition, although it is clear that scattering by phonons and defects will permit violation of this restriction. The sum over K_t may be converted to an integral[66]

$$\sum_{K_t} \rightarrow \frac{1}{(2\pi)^2} \int dk_y \; dK_z \rightarrow \frac{1}{2\pi} \int K_t \; dK_t$$

$$\rightarrow \frac{1}{2\pi} \quad \frac{m_t}{\hbar^2} \int dE_t \qquad 3.5.3$$

where $E_t = \dfrac{\hbar^2 \; K_t^{\;2}}{2m_t}$

Thus

$$J_x = \frac{2m_t q}{\hbar^3} \int_{-\infty}^{\infty} dE_x \int dE_t \left| M_{ab} \right|^2 \; \rho_a \rho_b (f_a - f_b) \qquad 3.5.4$$

and the limits on E_t must depend on configuration. For MIS diode the above expression is

$$J_x = \frac{2m_t q}{\hbar^3} \int_0^{\infty} \int_0^{E_{max}} \left| M_{sm} \right|^2 \; \rho_s \; \rho_m (f_s - f_m) dE_t dE_x \qquad 3.5.5$$

This expression deals with the forward current and assumes that tunneling through Schottky barrier is negligible (for moderate levels). The lower limit on these integrals (the zero of energy) can therefore be chosen as the semiconductor conduction band at the surface. This gives

$$\int_0^{\infty} \int_0^{E_{max}} dE_t \; dE_x \rightarrow \int_0^{E_{max} - E_x} \int_0^{E_{max}} dE_t \; dE_x \qquad 3.5.6$$

Since the Fermi functions in this relationship tend to zero with increasing energy, the upper limits on the integration are taken to be .

Using the WKB (Wentzel-Kramers-Brilloeen) method for the transmission coefficient

$$\left| M_{sm} \right|^2 = \left(\frac{\hbar^2}{2m}\right) \quad \frac{(K_x)_s}{L_s} \quad \frac{(K_x)_m}{L_m} \exp\left\{ -2\int_{x_s}^{x_m} \left| k_x \right| dx \right\} \qquad 3.5.7$$

and the one-dimensional density of states factor

$$\rho_{s,m} = \frac{m\, L_{s,m}}{\pi\hbar^2\, (K_x)_{s,m}} \qquad 3.5.8$$

where K_x is the component of momentum in the x direction, $L_{s,m}$ are the lengths of the semiconductor and metal, respectively, and x_s and x_m are the classical turning points, leading to

$$|M_{sm}|^2 = \frac{1}{\rho_s \rho_m} \frac{1}{(2\pi)^2} \exp\left(-2 \int_{x_s}^{x_m} |k_x|\, d_x\right) \qquad 3.5.9$$

A rectangular barrier is assumed of height W independent of x. $(W - E_x) \cong \chi$, the distance from the conduction band edge of the sami-conductor to that of the insulator. If follows that

$$K_x = \left(\frac{2m}{\hbar^2} (W - E_x)\right)^{\frac{1}{2}} \qquad 3.5.10$$

Also $x_m - x_x = \partial$, the film thickness. Thus

$$|M_{sm}|^2 = \frac{1}{\rho_s \rho_m} \frac{1}{(2\pi)^2} \exp\left(-\frac{4\pi}{\hbar}(2m\chi)^{\frac{1}{2}}\partial\right)$$

$$= \frac{1}{\rho_s \rho_m (2\pi)^2} \exp(-1.01\chi^{\frac{1}{2}}\partial) \qquad 3.5.11$$

where χ is expressed in electron volts and ∂ in angstroms. For forward bias, $f_m \cong 0$ and

$$f_s \cong \exp\left\{-(E_x + E_t - E_{fs})/KT\right\} \qquad 3.5.12$$

the Boltzmann approximation for non-degenerate materials. E_{fs} is the energy of the semiconductor Fermi level (relative to the zero of energy, which is the conduction band at the surface), Thus we have

$$J_x = \frac{m_t q}{2\pi^2 \hbar^3} \int_0^\infty \int_0^\infty \exp(-\chi^{\frac{1}{2}} \partial) \exp\left(-\frac{E_x + E_t - E_{fs}}{KT}\right) dE_x dE_t$$

$$= \frac{4\pi m_t q}{\hbar^3} \exp(-\chi^{\frac{1}{2}} \partial) \exp\left(\frac{E_{fs}}{KT}\right) \times$$

$$\int_0^\infty \int_0^\infty \exp\left(-\frac{E_x}{KT}\right) \exp\left(-\frac{E_t}{KT}\right) dE_x dE_t$$

$$= \frac{4m_t \pi q}{\hbar^3} (KT)^2 \exp\left(\frac{E_{fs}}{KT}\right) \exp(-\chi^{\frac{1}{2}} \partial) \qquad 3.5.13$$

where E_{fs} is negative since the Fermi level in the semiconductor is at a lower energy than the conduction band edge at the surface and is described by

$$E_{fs} = -q(V_{bi} + \varnothing_n) \qquad 3.5.14$$

Therefore,

$$J_x = \frac{4m_t \pi q}{\hbar^3} (KT)^2 \exp(-\chi^{\frac{1}{2}} \partial) \exp\left(-\frac{q}{KT}(V_{bi} + \varnothing_n)\right) \qquad 3.5.15$$

where V_{bi} represents the surface potential in the semiconductor, which is the difference in potential between the conduction band edge at the surface and in the bulk. $\varnothing_n$ is the Fermi potential relative to the conduction band edge in the bulk semiconductor.

The zero-bias value of the surface potential, V_{bio} is better known as the diffusion potential. Provided that contribution to n-value from other mechanisms (such as recombination currents) are very small, the change in the surface potential may be related to the applied voltage by

$$n = - V/\Delta V_{bi} \qquad 3.5.16$$

where ΔV_{bi} is the change in surface potential as a result of the applied bias V. This n-value applies for a current-voltage plot which is truly exponential. Thus

$$V_{bi} = V_{bio} + \Delta V_{bi} = V_{bio} - \frac{V}{n} \qquad 3.5.17$$

Making use of the zero-bias condition

$$V_{bio} + \phi_n = \phi_B \qquad 3.5.18$$

where ϕ_B is the barrier height presented to the electrons in the metal by the semiconductor alone, equation 3.5.15 becomes

$$J_x = AT^2 \exp(-\chi^{\frac{1}{2}} \delta) \exp\left(\frac{-q\phi_B}{KT}\right) \exp\left(\frac{qV}{nKT}\right) \qquad 3.5.19$$

where

$$A = \left(\frac{4\pi m_t q}{h^3}\right) K^2.$$

The equation 3.5.19 is valid only for forward bias $V > 3KT/q$ since the reverse current contribution (due to metal electrons tunneling into semiconductor) has been neglected.

3.6 EXPRESSION FOR CURRENT IN MIS SOLAR CELLS

The total current density produced by p-type MIS diode at a voltage V is given by an equivalent expression as equation 3.4.22.

$$J = J_L - T_v A^* T^2 \exp\left(\frac{-q\phi_{Bp}}{KT}\right) \times \left[\exp\left(\frac{qV_s}{KT}\right) - \exp\left(\frac{-qV_i}{KT}\right)\right]$$

$$- T_c \frac{n_{po} D_n}{L_n} \left[\exp\left(\frac{qV}{KT}\right) - 1\right] \qquad 3.6.1$$

The tunneling transmission probabilities are obtained in the previous section from WKB method and is approximated by

$$T_v \cong \exp\left(- \chi_p^{\frac{1}{2}} \partial\right) \qquad 3.6.2$$

where χ_p is the mean barrier height presented by the oxide layer for p-type material.

In short circuit condiction $V = I_{sc} R_s$ and the thickness dependence of I_{sc} can be visualized through finding the root of the equation 3.6.1.

In the Schottky barrier analysis the minority diffusion current can be neglected but it can be enhanced in the MIS diode due to accumulation of minority carrier in the interfacial layer. However, neglecting the voltage built in the insulating layer, i.e, $V_i \cong 0$, equation 3.6.1 can be reduced to

$$J = J_L - A^* T^2 \exp\left(-\chi_p^{\frac{1}{2}} \partial\right) \exp\left(\frac{-q\phi_{Bp}}{KT}\right) \times \left[\exp\left(\frac{qV}{KT}\right) - 1\right] \qquad 3.6.3$$

$$= J_L - J_o \left[\exp\left(\frac{qV}{KT}\right) - 1\right] \qquad 3.6.4$$

The open circuit voltage is obtained by putting $J = 0$ and with $J_L = J_{sc}$, we have

$$V_{oc} \doteq \frac{KT}{q}\left[\left[\ln \frac{J_{sc}}{J_{no}}\right] + \chi_p^{\frac{1}{2}}\, \delta\right] \qquad 3.6.5$$

$$\text{where } J_{no} = A^{*}\, T^{2}\, \exp\left(- \frac{q\emptyset_{Bp}}{KT} \right) \qquad 3.6.6$$

is the thermionic emission current density. The last term is responsible for the increase in V_{oc} due to interfacial layer.[54]

CHAPTER IV

FABRICATION OF SOLAR CELLS AND MEASUREMENTS

4.1 PRELIMINARIES

In this chapter the process of fabrication of Schottky barrier and Metal-Oxide-Semiconductor solar cells has been described. All of them were fabricated in Edwards-306 vacuum system coating unit fitted with a film thickness monitor having an accuracy of one angstrom. Metals and antireflecting coatings were deposited on cleaned surfaces of doped semiconductor wafer at a residual pressure of about 10^{-5} torr. P-type monocrystalline silicons of Monsanto Monex having resistivity of 1.5–3.5 ohm cm were used in the fabrication of solar cells. Fabrication of solar cells started with chemical cleaning of the silicon substrates having doped epitaxial layer. The current-voltage (I-V) measurements in dark and under illuminated conditions were performed. A X-Y plotter, oscilloscope, oscillator, power supply, digital multimeter were used in the measurement.

4.2 FABRICATION PROCESS

In the fabrication process the following steps were followed.

(1) Chemical cleaning of the substrate

(2) Preparation of ohmic contact

(3) Preparation of barrier metal contact

(4) Preparation of current collecting grids or fingers

(5) Deposition of antireflection coating

(6) Mounting and Lead connection.

4.2.1 Chemical Cleaning

The epitaxial layer side of the silicon substrates was originally polished. These were cleaned chemically where some variations were made e.g. some of them were slightly etched and some of them were not. We devide this cleaning step into two categories.

(a) --- Degreasing the substrate in methanol, acetone and ethyl alcohol.

--- Cleaning Ultrasonically in the same solution for 5 minutes.

--- Rinsing in distilled water for 15 minutes.

--- Rinsing in ethyl alcohol.

--- Drawing at 80°C in a drier.

(b) --- Degreasing the substrate in methanol, acetone and ethyl alcohol.

--- Ultrasonic cleaning.

--- Etching in the solution of 1 part hydrofloric acid, 5 parts, nitric acid by volume for 1-3 minutes or, etching in a solution of 48% hydrofloric acid for 1-3 minutes.

--- Rinsing in distilled water for 15 minutes.

--- Ultrasonic cleaning in ethyl alcohol for 3 minutes.

--- Drying at 80°C.

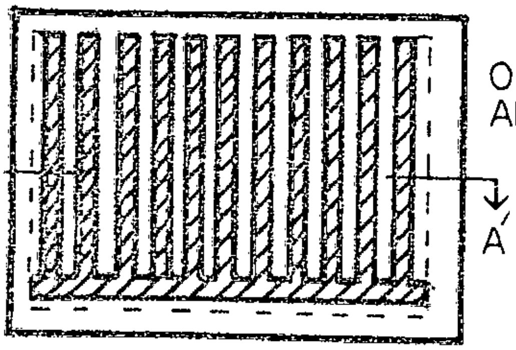

FIGURE (4.1a)
SCHEMATIC DIAGRAM OF SCHOTTKY BARRIER SOLAR CELL

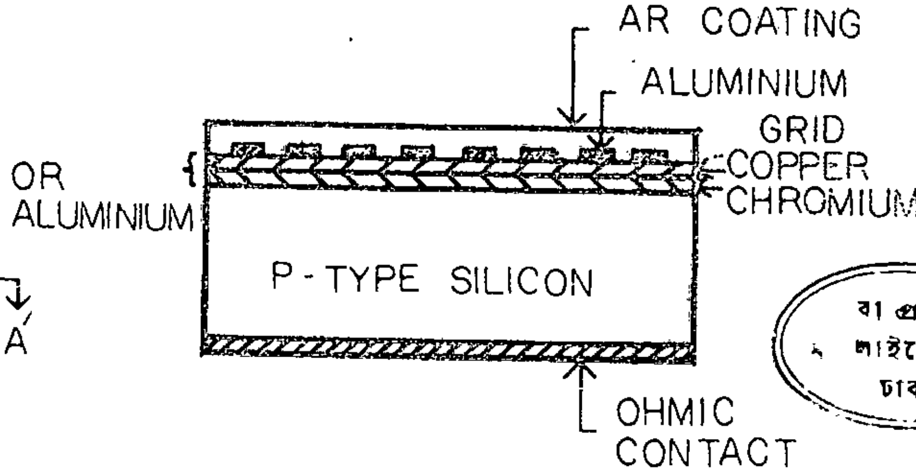

FIGURE (4.1b)
SECTIONAL VIEW THROUGH AA'

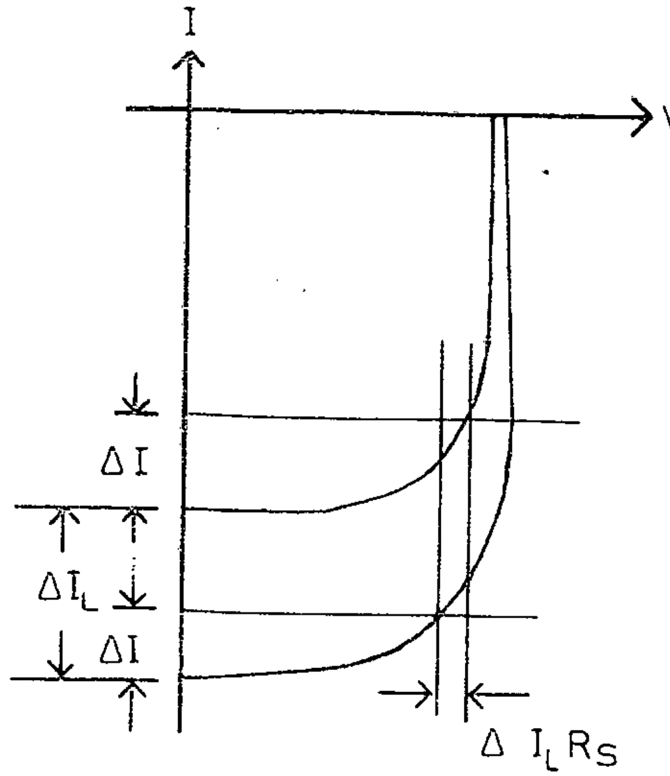

FIGURE (4.2) A METHOD FOR THE DETERMINATION OF THE INTERNAL SERIES RESISTANCES

4.2.2 Ohmic Contact

The silicon substractes were all p-type. The ohmic contact was obtained by depositing gold or aluminium on the rough side of the substrate at a residual pressure of 8×10^{-5} torr at a rate of 40-50 Å/sec. The samples were then heated in an open furnace for 5 minutes at $550^{\circ}C$ for gold contact and at $610^{\circ}C$ for 20 minutes for aluminium contact.

4.2.3 Deposition of Barrier Metal, Grid and Antireflection Coating

The general structure of the Schottky barrier and MIS solar cell fabricated is shown in Fig. 4.1(a,b). After alloying of the ohmic contact, the samples were further cleaned in a solution of acetone and ethyl alcohol to remove dirt particles from the polished active side. The silicon is supposed to contain a naturally grown oxide layer and alloying process further adds to its thickness. Also that in the cleaning process by aqueous solution the oxide formation continues. In the case of Schottky barrier this cleaning process is done for a very short period of time and the sample is put in the vacuum system to prevent further oxidation and to deposit the barrier metal. For metal-oxide-semiconductor (MOS) solar cell the samples were heated at different temperatures for different period of time and they were then rinsed in ethyl alcohol and acetone followed by drying at $80^{\circ}C$ before metal deposition.

Now a mask of aluminium foil was placed on the active surface keeping a window for deposition of barrier metal contact.

This was done in order to prevent any deposition of metal on the edge of the silicon substrate, other-wise edge leakage current would worsen the value of shunt resistance R_{sh}. Then the desired metal/metals of appropriate thickness was deposited at a residual pressure of 4×10^{-5} torr.

Above the Schottky metal contact, aluminium fingers or current collecting grids were deposited by the help of another mask made of aluminium foil, thick plastic, comb etc. Finally an antireflection (AR) coating of ZnS was deposited throughout the surface of the device leaving a very small area of aluminium grid exposed, which is required for the connection of external leads. The list of solar cells fabricated are given in Table 4. in which every details of fabrication have been shown.

4.2.4 Mounting and Lead Connection

The solar cells fabricated were then attached to copper plates by silver conducting pastes. Wires were also connected to the top aluminium grid.

4.3 MEASUREMENT

Current-voltage measurements (I-V) were performed on the Schottky barrier diode in order to find out the parameters e.g. barrier height, ϕ_B, dark saturation current I_o, ideality parameter n, series resistance R_s, short circuit current I_{sc}, open circuit voltage V_{oc} and fill factor FF. These measurements were done in dark and also in illuminated conditions. The value of

TABLE 4

Sl. No.	Device No.	Area: Actual cm^2	Area: Effective cm^2	Cleaning method	Ohmic contact Å	Oxidation temp. °C -hr.	Barrier metal Å	Finger: Spacing/width cm	Finger: Thickness Å	AR Coating Å	Type of cell
1	S1	0.8	0.3	a	Au 1000	×	Cr/Cu 550/500	0.1/0.1	500	1000	Schottky
2	S2	0.9	0.3	a	Au 1000	×	Cr/Cu 60/60	0.1/0.1	500	650	Schottky
3	S3	0.7	0.4	b	Al 1000	150/48	Al 120	0.1/0.1	1000	650	MIS
4	S4	0.9	0.4	b	Al 1000	150/96	Cr/Cu 60/50	0.2/0.1	1000	650	MIS
5	S5	1.0	0.5	b	Al 1000	150/144	Cr/Cu 60/50	0.1/0.1	1000	650	MIS
6	S6	0.95	0.4	a	Al 1000	150/48	Cr/Cu 35/50	0.1/0.1	1000	650	MIS
7	S7	0.9	0.7	a	Al 1000	150/72	Al 130	0.2/0.1	1000	650	MIS
8	S8	0.95	0.3	b	Al 1000	×	Al 120	0.1/0.1	1000	650	Schottky
9	S9	0.6	0.5	b	Au 1000	150/96	Cr/Cu 35/50	0.2/0.05	1000	650	MIS
10	S10	0.9	0.7	a	Au 1000	150/144	Cr/Cu 60/50	0.2/0.1	1000	600	MIS

barrier height $\emptyset_B$ and ideality parameter, n can be obtained from the plot of Log I Vs V in forward direction according to the following equation 4.3.1. Log I Vs. V plots were straight lines.

$$\emptyset_B = \frac{KT}{q} \ln \left(\frac{SA^{**} T^2}{I_o} \right) \qquad 4.3.1$$

$$\text{and } n = \frac{q}{KT} \frac{\partial V}{\partial (\ln I)} \qquad 4.3.2$$

The effective Richardson's constant A^{**} is function of electric field at the interface. In the range of electric field of 10^4 to 2×10^5 V/cm, A^{**} is given by

$A^{**} = 115 \ amp/cm^2/^oK^2$ for electrons

$= 30 \ amp/cm^2/^oK^2$ for holes

4.3.1 Current Voltage Measurement

I-V measurements was performed on the diode both in the forward and reverse directions. These were obtained by X-Y plotter or digital multimeter. The forward characteristics were drawn in dark and illuminated condition. The value of the barrier height $\emptyset_B$, ideality parameter n and the value of dark saturation current was obtained from the flot of log I Vs.V in the forward direction with the help of equations 4.3.1 and 4.3.2.

Three types of I-V characteristics can be obtained from the solar cells (Appendix-B) They are

i) Photo-voltaic output characteristics.

ii) Diode forward characteristics

iii) p-n junction characteristics.

The diode forward characteristics was obtained for all the cells. The photovoltaic characteristic was however useful to find the internal series resistance. From the knowledge of this internal series resistance the actual diode characteristic was obtained from the diode characteristic by using the following equation 4.3.3. At any current, the voltage across the diode is given by

$$V' = V - IR_s \qquad 4.3.3$$

4.3.2 Internal Series Resistance Measurement

For easy and accurate measurement of internal series resistance(67) of the solar cell photovoltaic output characteristic is measured at two different light intensities, the magnitudes of which are not very importance. The two characteristics are translated againsts each other by the amount ΔI_L and $\Delta I_L R_s$ in y-and x-directions, respectively (Appendix-C). Two corresponding point on the two characteristic show a displacement with respect to each other which same as the two translation of coordinate system. The displacement parallel to the ordinate gives the value of ΔI_L and the displacement parallel to the abscissa equals $\Delta I_L R_s$ from which the value of R_s is readily obtained.

In this method an arbitrary interval ΔI from the short circuit current I_{sc} is chosen on both the characteristics. This methods locates the corresponding points on the two curves. It is convenient to choose ΔI so as to obtain a point in or near the knee of the characteristic. An illustration of the procedure is shown in Fig. 4.2.

CHAPTER V

RESULTS AND DISCUSSIONS

RESULTS AND DISCUSSIONS

Two types of solar cells were fabricated in the micro-electronics laboratory of Electrical Engineering Department, BUET — Schottky barrier (S1, S2, S8) and metal-oxide semiconductor (S3, S4, S5, S6, S7, S9, S10) solar cells. The metal contacts were aluminium and chromium/copper. The backside Ohmic contact was gold or aluminium. The current voltage (I-V) curves of the devices fabricated are given in Figs. 5.1 to 5.9. These curves are derived in dark and also under illuminated conditions. Barrier height, ϕ_B ideality parameter, n, dark saturation current, I_o, open circuit voltage, V_{oc}, short circuit current, I_{sc} and value of series resistance, R_s can be obtained from these plots. The intercepts and slope of the straight line extrapolation of the plot of Log I Vs. V (Fig. 5.10, 5.11) in the forward direction determine the dark saturation current and ideality parameter. The various results obtained for the cells are tabulated in Table 5.

Device S1 is a Schottky barrier solar cell. The metal contact is very high (550/500 Å) and therefore, it showed a very small value of short circuit current density (0.83 mA/cm^2). Device S2 is also a Schottky barrier solar cell. The increased current (8.34 mA/cm^2) may be explained as a consequence of decreasing the barrier metal thickness (60/60 Å). The open circuit voltage is comparatively large (0.368 volts). This sample was cleaned by method a) and there was probably an interfacial oxide layer already present on its surface.

TABLE 5

Sl. No.	Device No.	Dark Saturation current ua	Dark Saturation current density ua/cm^2	Barrier height volts	Ideality parameter	Series resistance Ohm	Short circuit current mA	Short circuit current density mA/cm^2	Open circuit voltage	Maximum efficiency %	Fill factor
1	S1	279	348	0.586	2.03	12	0.25	0.83	0.139	-	-
2	S2	232	257	0.601	2.3	20	2.5	8.34	0.368	1.15	0.38
3	S3	32	45.7	0.652	2.14	19	4.0	10.0	0.27	1.0	0.38
4	S4	237	263	0.6	3.03	27	3.6	9.0	0.38	1.2	0.36
5	S5	63.2	63.2	0.638	3.87	70	2.5	3.5	0.467	0.77	0.34
6	S6	236	248	0.602	3.01	25	4.0	10.0	0.49	2.38	0.39
7	S7	35	39	0.65	2.61	25	4.5	6.4	0.371	1.03	0.445
8	S8	151	215	0.606	2.42	12	2.0	6.7	0.238	0.62	0.40
9	S9	157	262	0.601	3.38	17	6.0	12.0	0.421	2.17	0.39

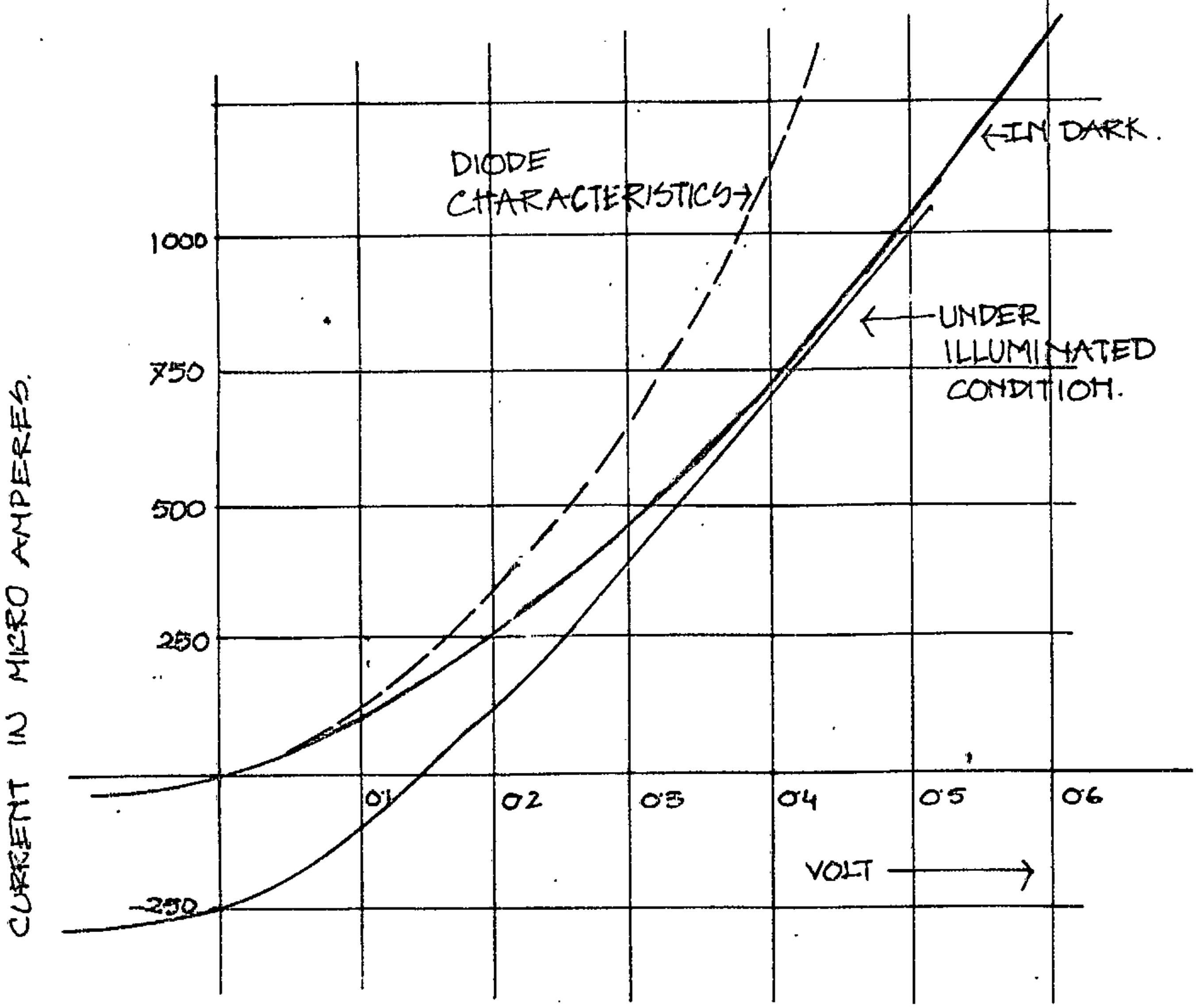

FIGURE — 5·1
CURRENT VOLTAGE (I-V)
CHARACTERISTICS OF SOLAR CELL S_1

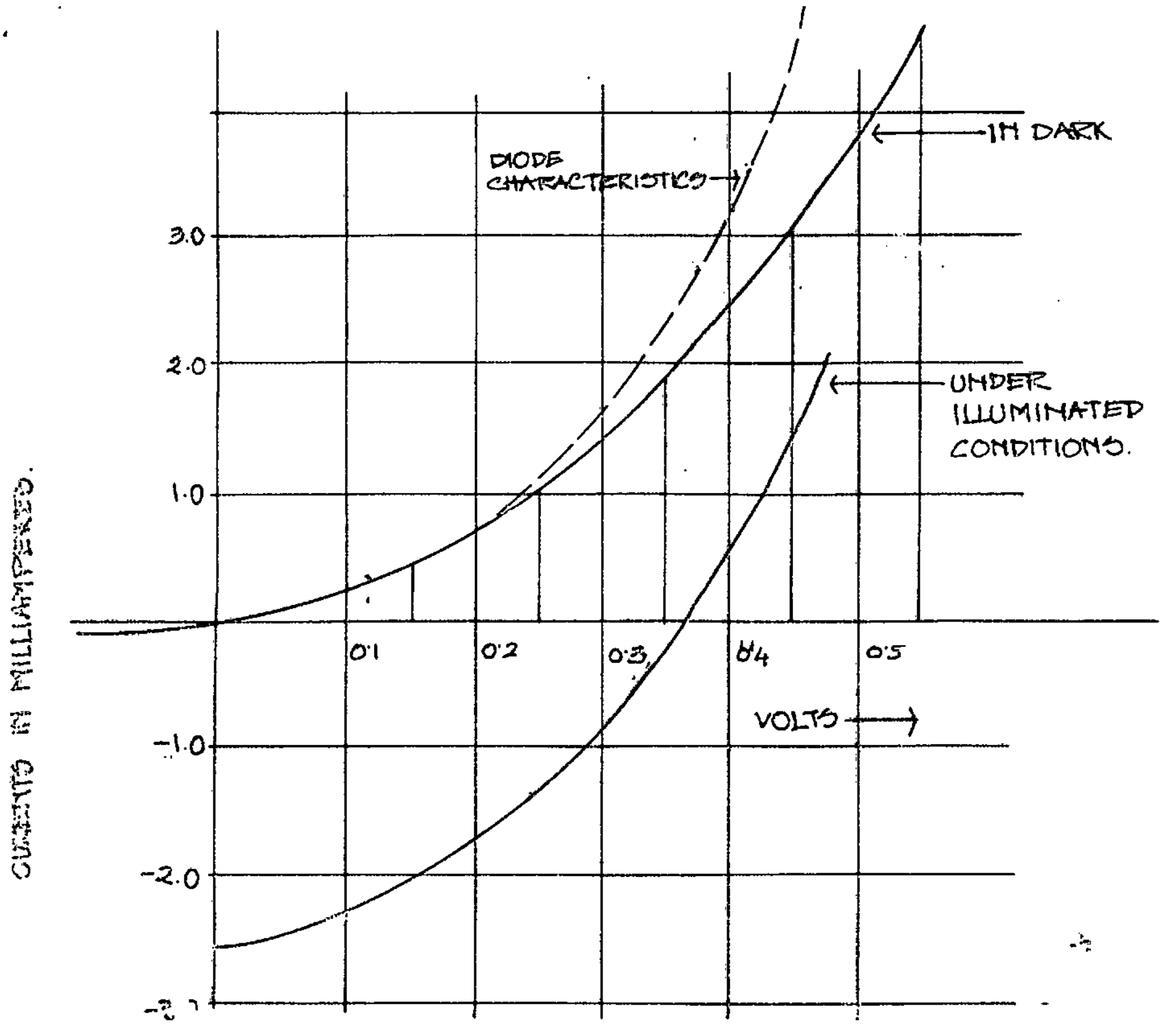

FIGURE — 5.2

CURRENT-VOLTAGE (I-V) CHARACTERISTICS FOR SOLAR CELL S_2.

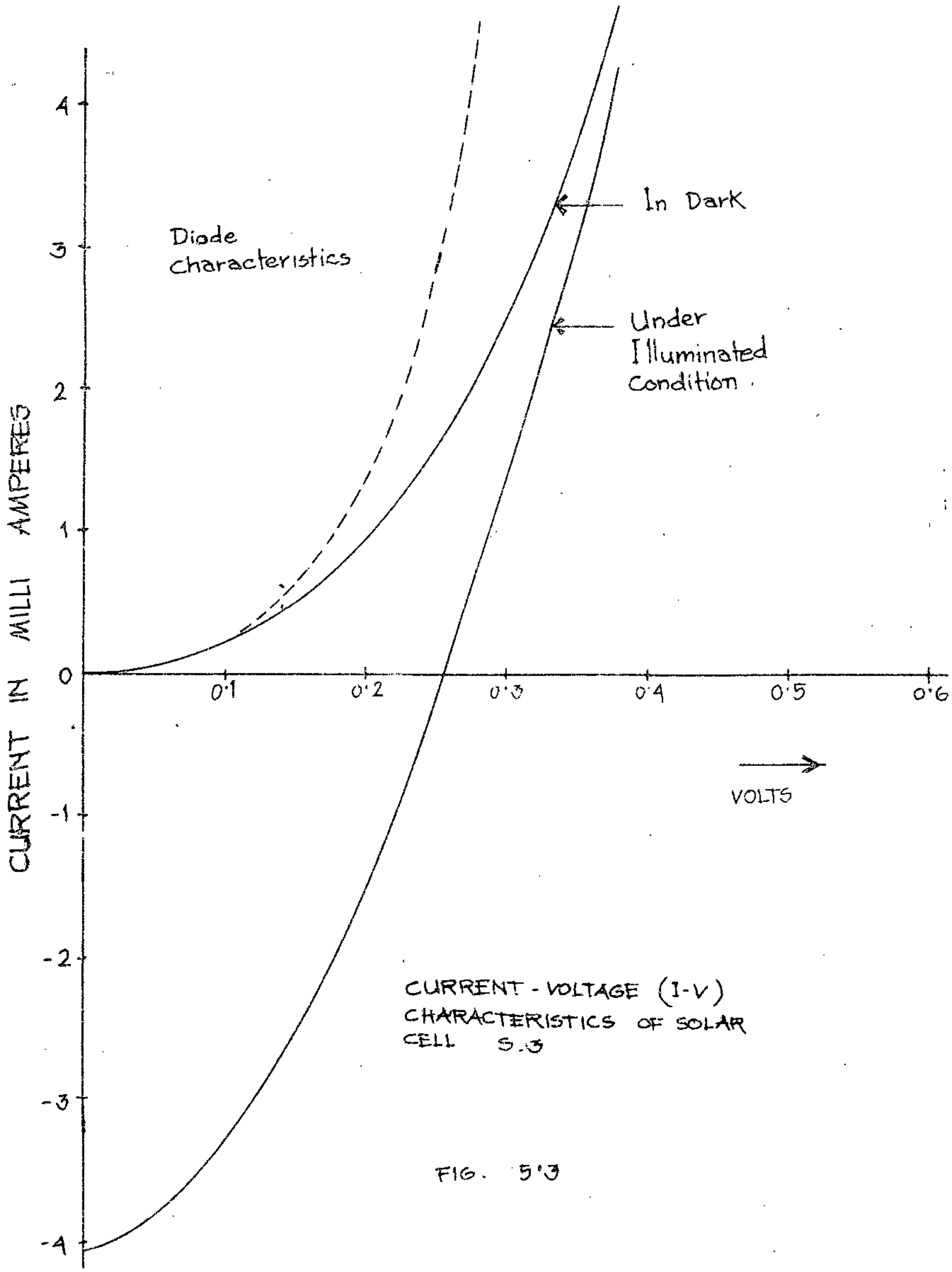

CURRENT IN MILLI AMPERES
4
3
2
1
0
-1
-2
-3
-4
0·1
0·2
0·3
0·4
0·5
0·6
VOLTS
Diode Characteristics
In Dark
Under Illuminated Condition.
CURRENT - VOLTAGE (I-V) CHARACTERISTICS OF SOLAR CELL 5.3

FIG. 5·3

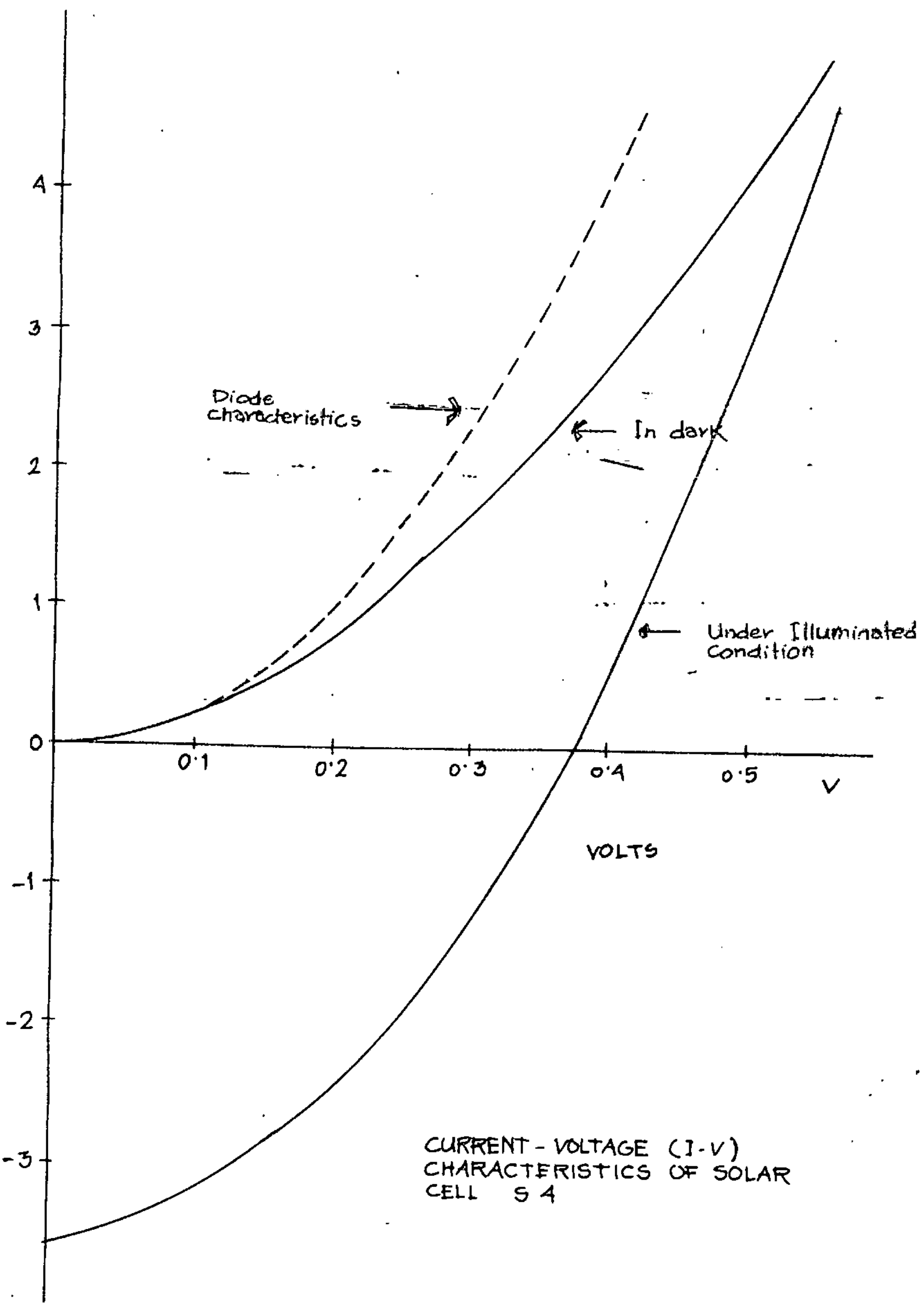

CURRENT - VOLTAGE (I-V) CHARACTERISTICS OF SOLAR CELL S 4

FIG. 5·4

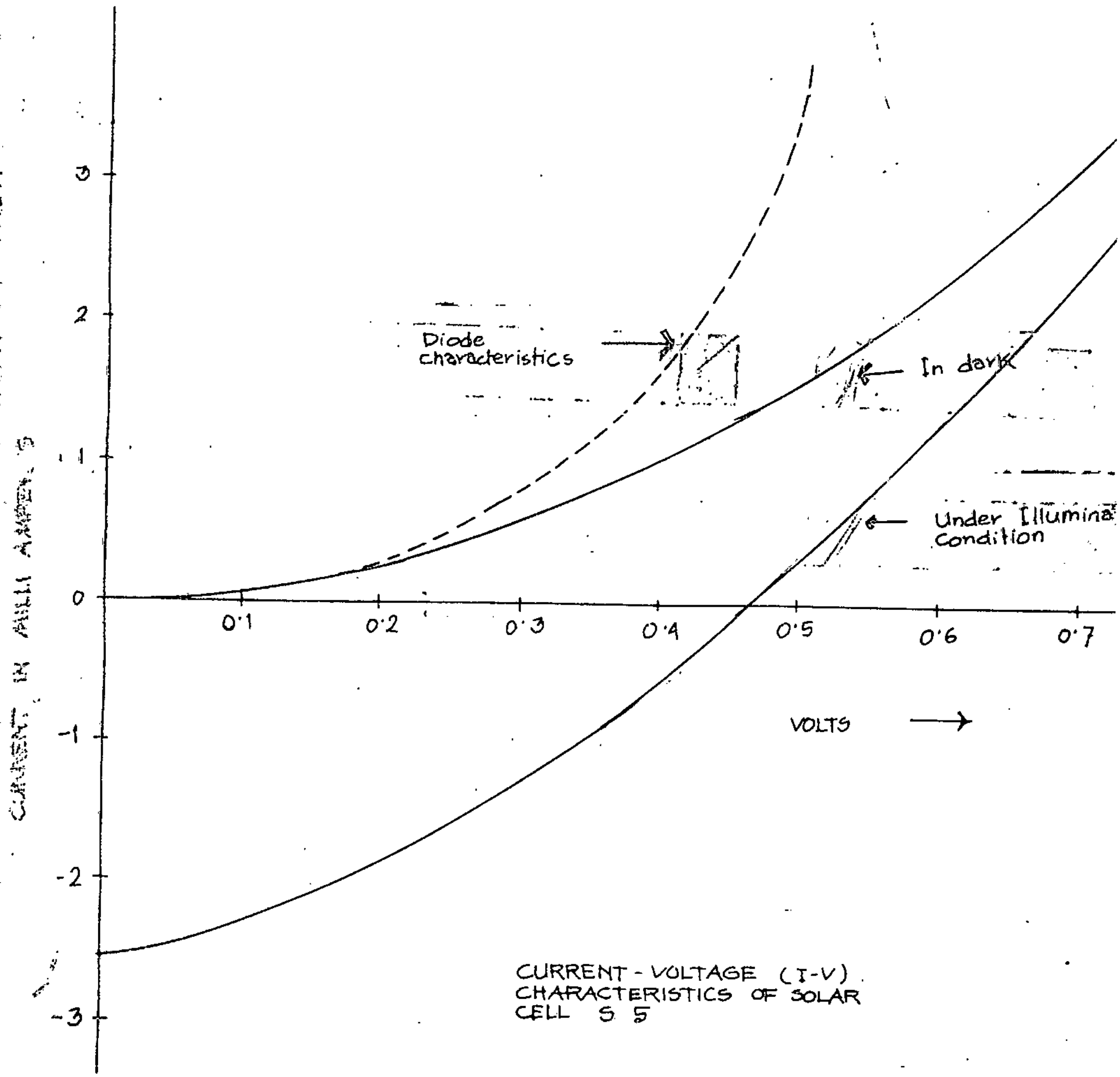
CURRENT IN MILLI AMPERES
3
2
1
0
-1
-2
-3
0·1
0·2
0·3
0·4
0·5
0·6
0·7
VOLTS
Diode characteristics
In dark
Under Illumina condition
CURRENT - VOLTAGE (I-V) CHARACTERISTICS OF SOLAR CELL S 5

FIG. 5·5

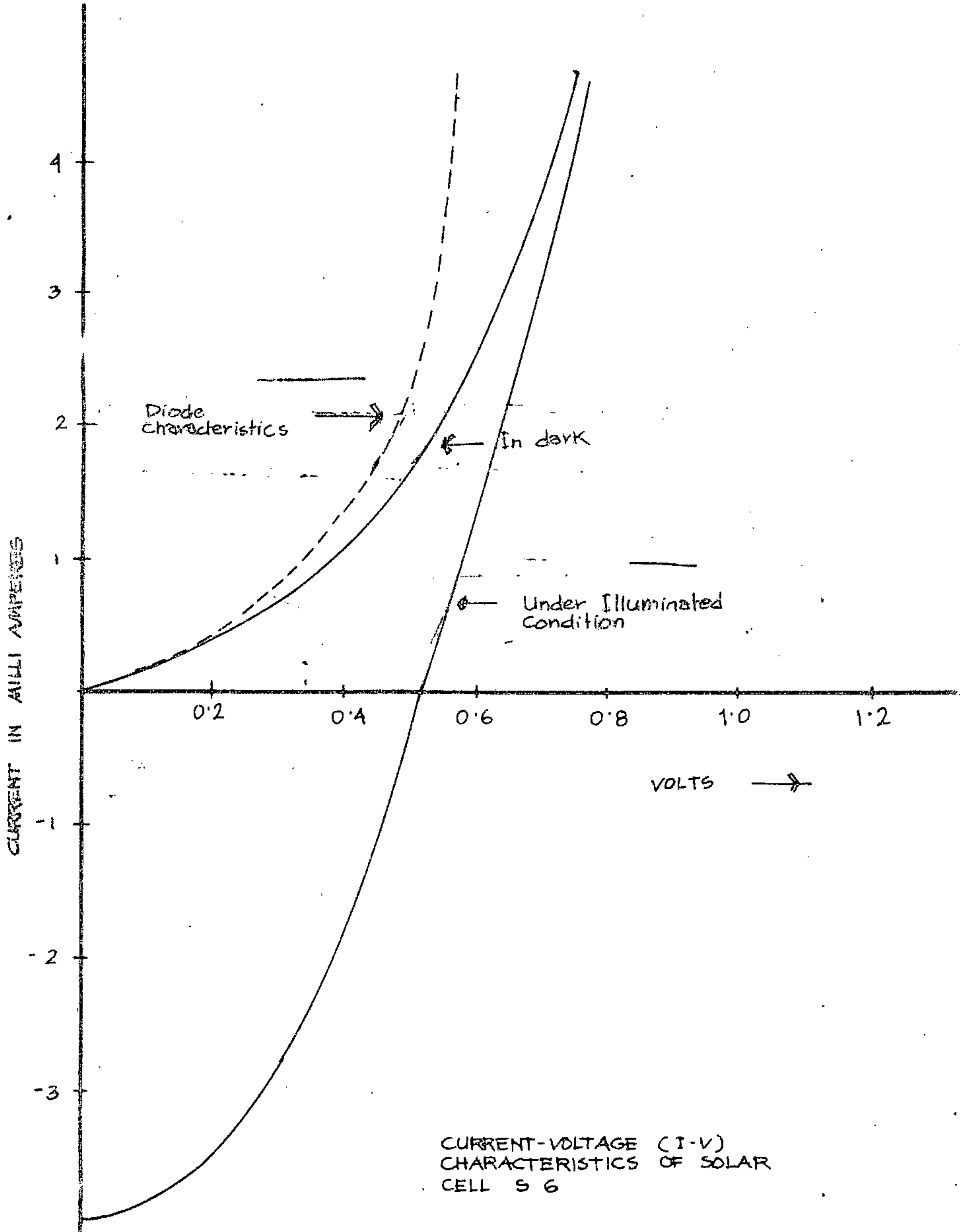
Diode characteristics
In dark
Under Illuminated Condition
CURRENT IN MILLI AMPERES
VOLTS
0·2
0·4
0·6
0·8
1·0
1·2
4
3
2
1
-1
-2
-3
CURRENT-VOLTAGE (I-V) CHARACTERISTICS OF SOLAR CELL S 6

FIG. 5·6

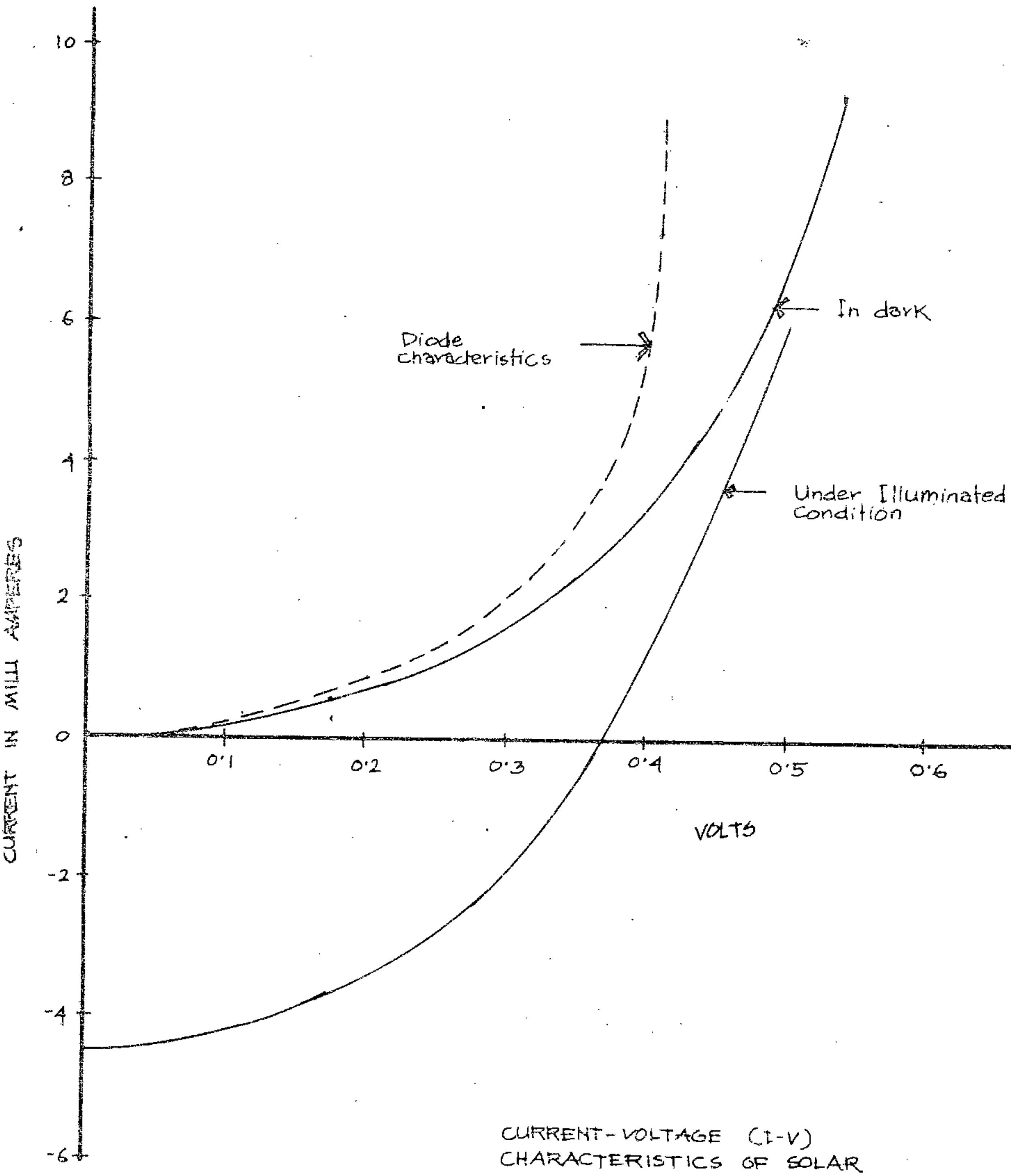

CURRENT-VOLTAGE (I-V) CHARACTERISTICS OF SOLAR CELL S 7

FIG - 5·7

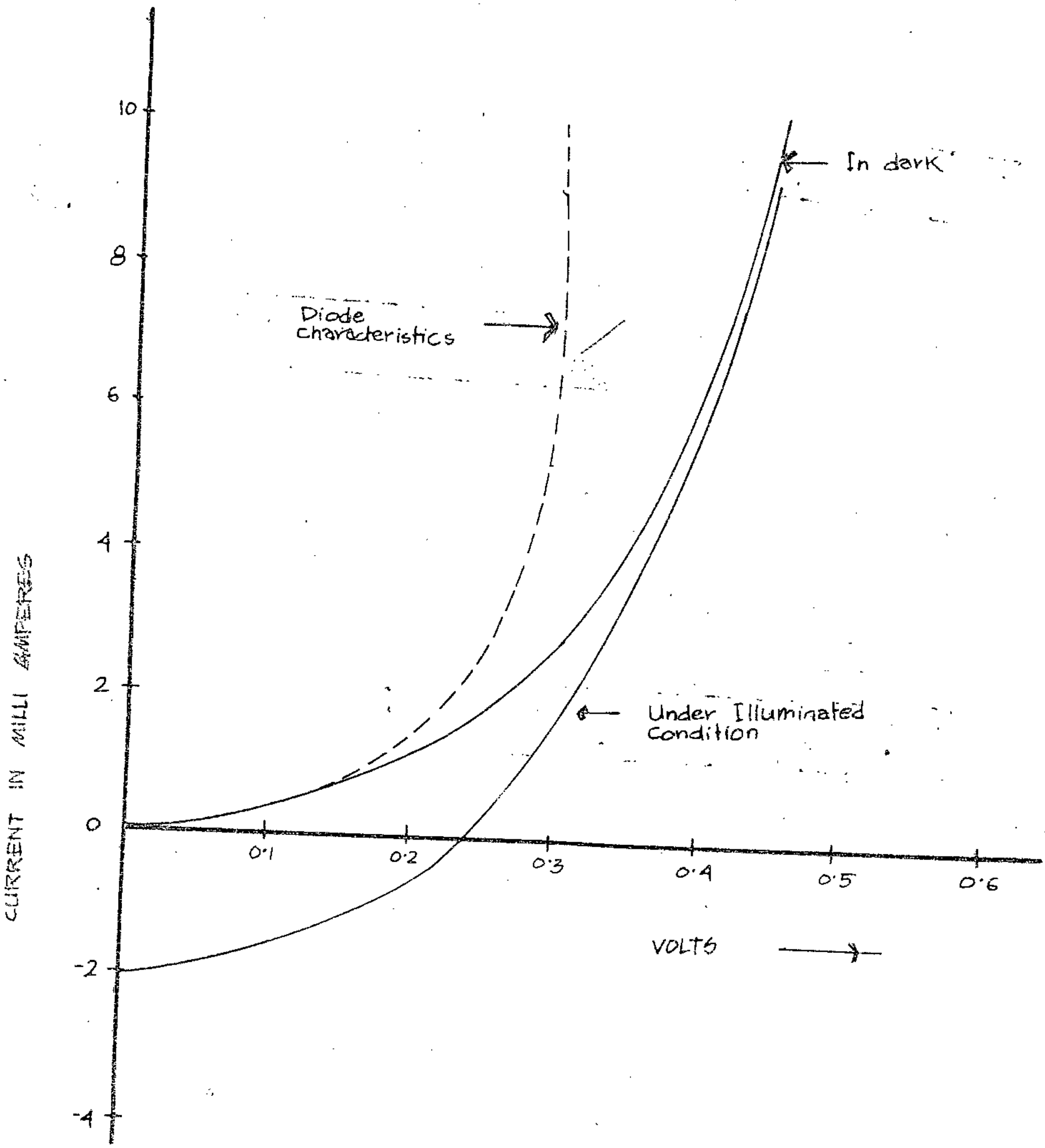

CURRENT - VOLTAGE (I-V) CHARACTERISTICS OF SOLAR CELL 5-B

FIG - 5·8

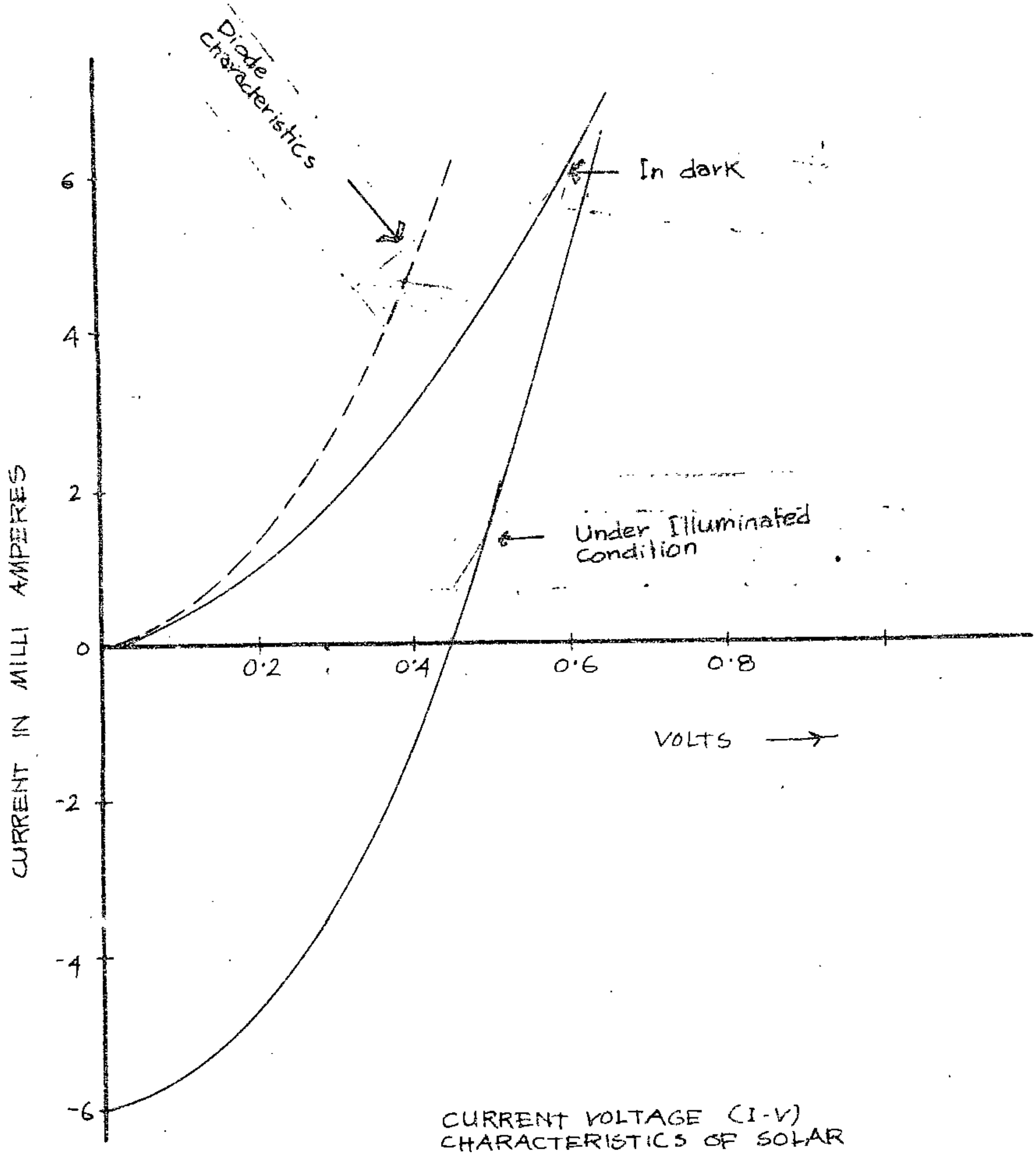

CURRENT VOLTAGE (I-V) CHARACTERISTICS OF SOLAR CELL 5 9

FIG. 5-9

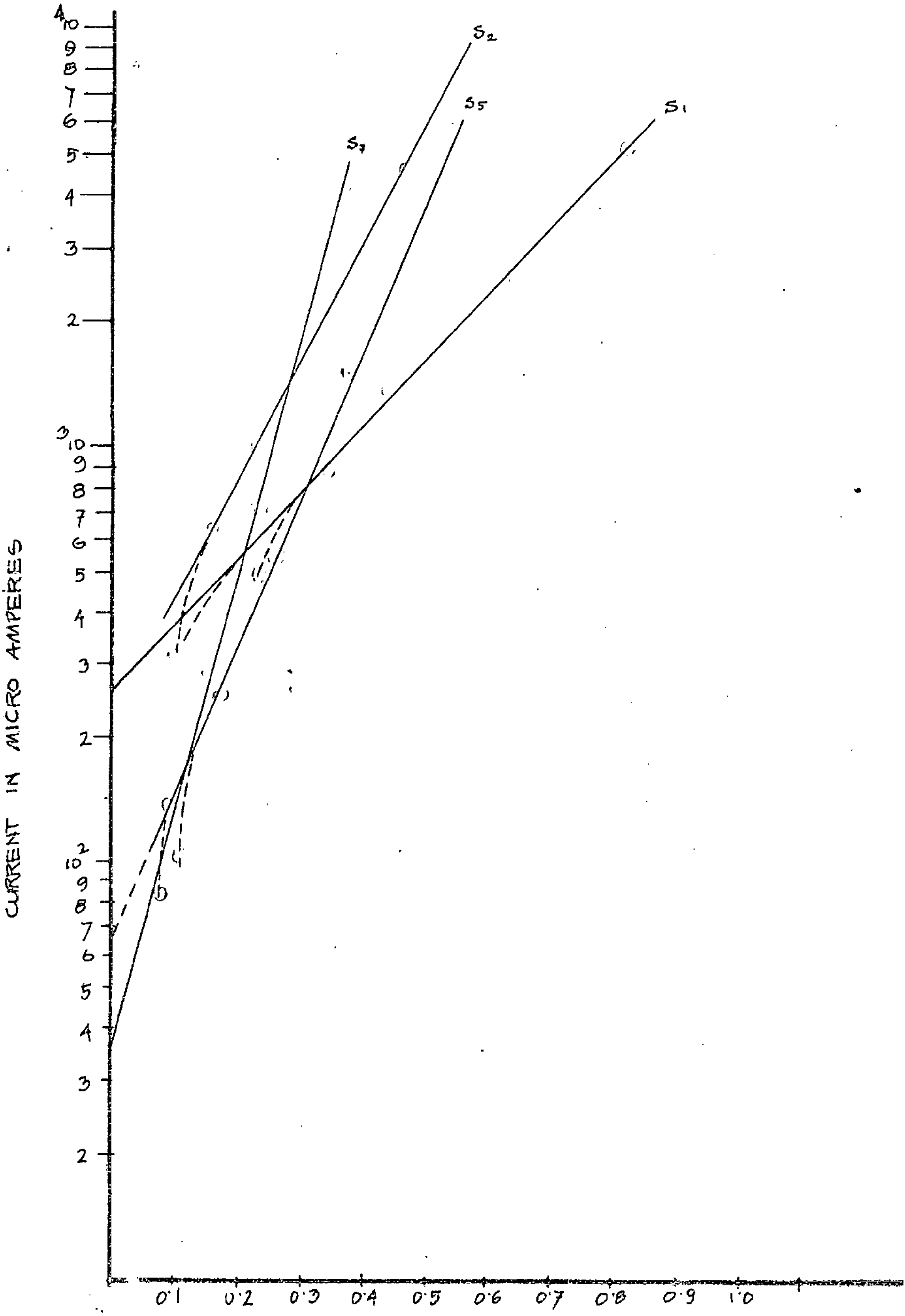

FIGURE 5·10

LOG I VS V CURVES OF DEVICES

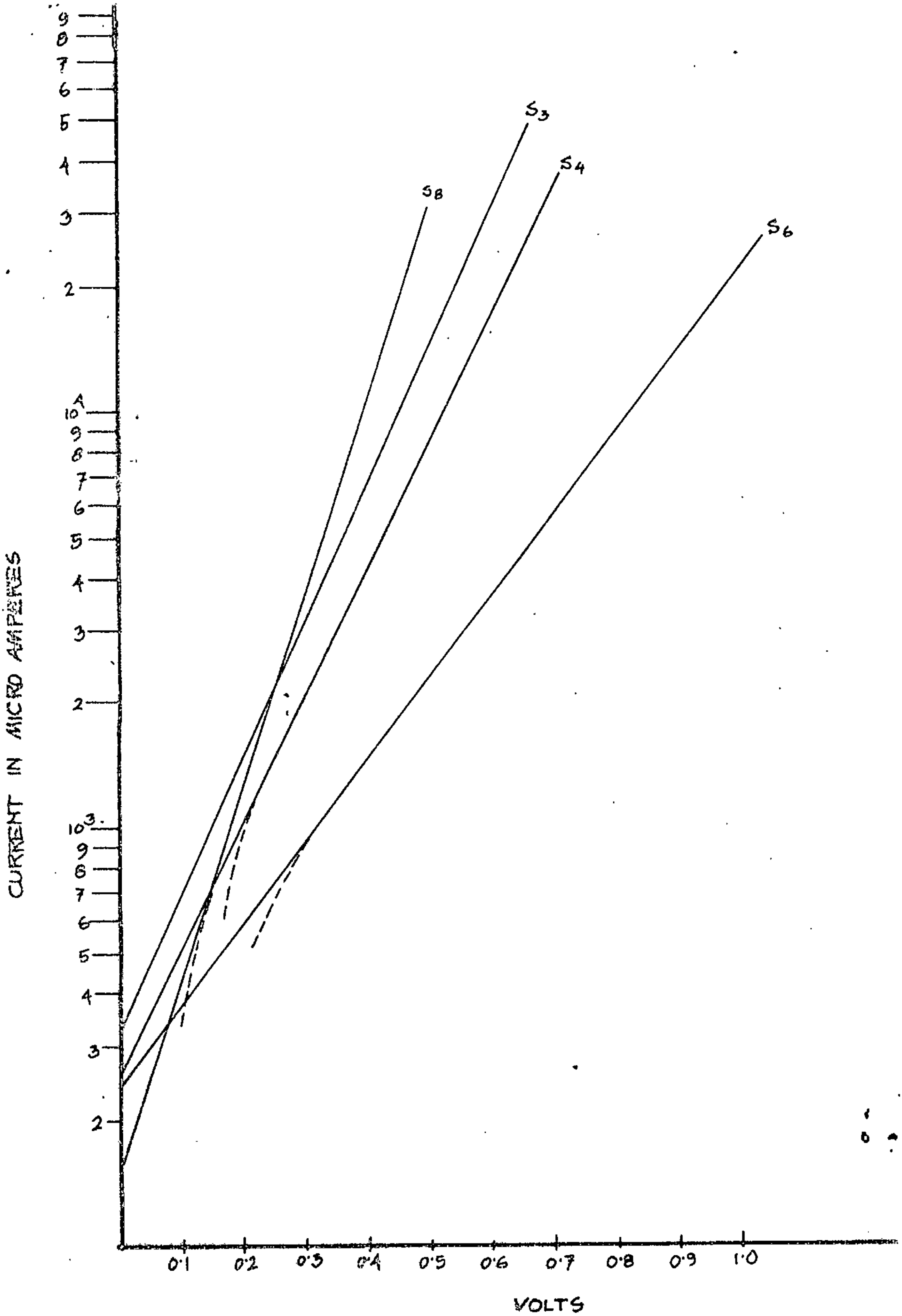

FIGURE 5·11 LOG I VS V PLOT OF DEVICES

Devices S3 and S7 are aluminium MIS solar cells. S3 was heated at $150^{\circ}C$ for 48 hours and S7 was heated for 72 hours. There is a rise in the value of open circuit voltage (0.371 volts for S7). Although the effective area for S7 is higher than that of S3, the resistance value for S7 was higher. As a result the short circuit current density for S7 is lower ($6.4\ mA/cm^2$) in comparison with the current of device S3 ($10.0\ mA/cm^2$). This decreased current density is due to an increased oxide thickness and increased resistance value. Also device S7 was cleaned by method a). The high value of resistance (25 ohm) may be due to the increased spacing between the grids.

Devices S4 and S5 are also MIS cells. S5 shows a very high value of internal series resistance (70 ohm). S4 and S5 was oxidezed at $150^{\circ}C$ for 4 days and 6 days respectively. The barrier height for S5 is large (0.638 volt) but there is a photocurrent suppression and as a consequence the short circuit current is smaller ($3.5\ mA/cm^2$) than that of S4 ($9.0\ mA/cm^2$). The open circuit voltage was, however, large for S5. (0.467 volts).

The device S6 was heated for 48 hours at $150^{\circ}C$ and the barrier metal thickness was also decreased (35/50 Å). The short circuit current density increased ($10\ mA/cm^2$) and the open circuit voltage also showed a high value (0.49 volts). The cleaning was done by method a).

Device S8 is an aluminium Schttky solar cell. It was cleaned by method b). The resistance value is smaller (12 ohm) in comparison with that devices S3 (19 ohm) and S7 (25 ohm). The high value of resistance for S3 and S7 may be attributed to high value of interfacial layer thickness.

It has been found that if the samples are cleaned by method b) the initial oxide layer is removed. This gives a greater control in the fabrication of cell if reproducable cells are to be made. Device S9 was cleaned by method b) but heated for 4 days at $150^{o}C$. This cell the has shown almost the same performance as cell S6 although it had higher grid spacing. This cell was reproduciable and two more cells were fabricated which almost showed similar results. But device S6 was not strictly reproducible. The variation in performance was greater in comparison to those of devices S9.

In order to obtain high value of open circuit voltage V_{oc} a thin insulating oxide layer was grown on the silicon substrates. The fact that successful silicon cells utilize p-type material and not n-type for which the barrier heights are generally higher can be explained when the presence of interfacial layer is recognized. This layer contains positive charge which increases barrier height for p-type material. In order to fabricate MIS solar cells, simple heat treatment techniques were used.

In general, the insulator growth method used in MIS solar cell fabrication must provide in a reproducible, thin, stable insulating layer. In the fabrication process this was done by heating the substrates at $150^{o}C$ in air for 24 to 120 hours in an oven. In these results the short circuit current density J_{sc} is also an important quantity in determining the performance of the cell. J_{sc} depends upon the thickness and type of anti-reflection coating, thickness of oxide interfacial layer and reflection properties of the barrier metal. It also depends on the thickness of barrier metal, value of ideality parameter, dark saturation current alongwith the barrier height and also on the value of series resistance. In order to obtain higher efficiencies in MIS cells it is also important to have high value of short circuit current density. The first requirement to obtain high current is to use thin insulating layer so that photocurrent suppression effects are avoided. For silicon oxide, thickness less than 25 Å are required. In our process it was not, however, possible to determine the thickness of oxide interfacial layer. Therefore, strictly speaking it was not possible to have a complete control on the formation of oxide layer by simple heat treatment technique.

As found in literature(61) the interface of thermaly grown silicon reveals the existance of a transition region with composition of SiO_x, where x varies from one to two in the transition layer. This nonstoichiometric region extends to about 20 Å from the interface. Since the MIS solar cell involves ultrathin oxides (10 - 20 Å), the oxide thickness is comparable to the nonstoichiometric transition region. Therefore, the device performance is expected to be dependent on the composition of the oxide also. In addition, as the ultrathin oxide of 10 - 20 Å consists of only few atomic layers, it is expected to be heavily defected with a large pinhole density, therefore, the device performance will also depend on the quality of this oxide. The cells fabricated in our laboratory verified the fact that oxide layer grown in this technique was not uniform over the whole area. Solar cell S10 was fabricated using the same MIS technique. The area of the cell was 0.7 cm^2. The shot circuit current was only 50 microamperes. The solar cell was then cut into different small pieces. One of the pieces having an area of 0.04 cm^2 showed a short circuit current of 220 microamperes while another having an area of 0.06 cm^2 showed 155 microamperes. The open circuit voltages of the pieces were 0.3 and 0.17 volts respectively, while the open circuit voltage of the cell S10 was only 0.23 volts. The above situation can be visualized as if there are several solar cells in parallel combination, some of them having a large barrier height and others a smaller barrier height. Thus the region with minimum pinholes shows MIS structure while the region where pinhole density is so large that there is virtually no oxide can be considered as a Schottky structure. The parallel combination of ideal MIS and Schottky cells therefore, gives a low open circuit voltage and a considerable amount of photo-generated current is lost as internal diode current in the region of Schottky barrier.

The ideality parameter n of the cells were higher than that of near ideal values. (Table 5). This increased value of n is attributed to fixed charges in the oxide thickness. The ideality parameter is also a function of oxide thickness ∂ and surface state density D_s.

The conversion efficiency of the solar cell is given by

$$\eta = \frac{J_{sc} V_{oc} FF}{P_{in}}$$

where FF is given by the ratio $V_{mp} I_{mp}/V_{oc} I_{sc}$. From the I-V curves it is evident that the horizontal segment of the curves is very small. But this decrease in horizontal segment did not affect the open circuit voltage, therefore, the FF decreases with a subsequent decrease in efficiency. The fill factors FF shown in Table 5 is a consequence of high value of series resistance.

There are various reasons for this high value of series resistance. One of these is the back side ohmic contact. Aluminium ohmic contacts were selected with an aim to fabricate low-cost solar cells. The ohmic contact was annealed in air or in a chamber at a residual pressure of 10^{-2} torr. Ohmic contacts made of aluminium on p type silicon with heat treatment gives low value of barrier height. But in the presence of oxide layer which normally contains positively charged sodium (Na^+) and potassium (K^+) ions, the barrier heights were not low enough not to be distinguishable from a truly ohmic contact with no potential barrier at the interface. Moreover, heat treatment of this contact oxidized the aluminium which increased the resistivity of the metal contact. Heat treatment in vacuum, at a pressure of 10^{-2} torr and a temperature of $300^{0}C$ for a time of 5 minutes gives good results for aluminium contacts.

Another important contribution to the series resistance is from the transverse sheet resistance of the active metal contact on the top. Proper design of grid structure can theoretically reduce its value to a very low figure. Grids were made by evaporating aluminium through masks made of combs and aluminium foil. These masks were prepared by cutting the foil with a pair of scissors. The width of the grid lines could not however, be made less than 0.05 - 0.1 cm. The distance between the grid lines or fingers was varied from 0.1 cm to 0.5 cm. For smaller distance the value of the resistance contributed by the metal sheet decreases very rapidly but the effective area also decreased, thus decreasing the value of photogenerated current. With greater distance between the grids lines the resistance showed a very high value(S4,S7). Due to transverse current flow there is a voltage gradient existing between the grid lines. Under short circuit conditions regions of cell away from the contact strips remain under forward bias. Thus a considerable amount of current generated is lost as is evident from the equivalent circuit. For a particular dimension of cell if the separation of grids were decreased smaller amount of current of one unit field would have flowed through a much decreased resistance and as a consequence the forward bias voltage of the diode would be decredsed. But this improvement was not fully achieved because it reduced the effective area causing decrease in short circuit current density. A computer program has been run (Sec. 2.8) which verifies the above results.

In addition to these resistances there were other factors which contribute to the total resistance. These include conducting paints used for connecting electrodes, leads, copper plate on which cells were attached and the resistances of the measuring instrument (milliammeter). It has been determined that these resistances are approximately 4-5 ohm.

Another important factor which determines the value of J_{sc} (or J_L) is the antireflection coating. Aluminium is well known for its high reflectivity in the optical spectrum. Thus to make an efficient light conversion device some methods of maximizing the film transmittance had to be done. The same situation exists in the case of Cr/Cu solar cells. To decrease the reflection losses, antireflection coatings were used. The coating material was Zinc sulphide. A thickness of 600-700 Å showed good results for both type of solar cells. However, a simple inspection shows that there was still considerable loss from reflection at the top as is evident by its shining surface.

The efficiency calculations were done by assuming that the imput power density is 0.103 watts/cm^2. However, data obtained from Department of Mechanical Engineering showed that it varied from 0.92 to 0.101 Watts/cm^2 during that time. The efficiency calculations are tabulated so that an approximate idea about the performance of these cells can be made.

CHAPTER VI

CONCLUSIONS AND RECOMMENDATIONS

CONCLUSIONS AND RECOMMENDATIONS

The fabrication of Schottky barrier and MIS photovoltaic cells is a very sophisticated process which involves accurate control over all parameters if reproducible cells of good performance are to be made. In our fabrication process it was possible to obtain precise controlled thickness of different deposited layers on the silicon substrate. But there was vircually no control on the thickness of oxide interfacial layer on silicon. Oxide layer grown by our technique was not uniform as discussed in Chapter-5. This resulted in a decrease in short circuit current for cells having larger dimensions. Besides, the cells were not strictly reproducible.

In the process of fabrication aluminium masks or combs were used to fabricate the grids lines. The geometry of this grid is very important as discussed earlier. It is, therefore, essential to have masks which have been so made that the grid structures have very small width, so that the effective area is not decreased.

From the results obtained so far, it can be suggested that if the facilities of photolithography, photoresist process, oxide thickness measuring instrument, standard lamp sources and furnace with controllable environment were used, solar cells with higher efficiencies could be made.

It is also suggested that research and development should be continued and significant improvements can be done if elaborate computer study for the optimization of all parameters is done. This should be followed by fabrication with accurate control of the process. We have used monocrystalline silicon in our cells. But monocrystalline silicon substrates are more expensive than amorphous silicon. In order to make a cost effective solar cell works should also be done with amorphous or polycrystalline silicon. Besides silicon, investigation should be carried out with Cadmium sulphide, Galium Arsenide etc.

It is also suggested that fresh silicon substrates that are suitable for solar cell should be used for producing solar cells, otherwise, there will be virtually no control on the thickness of oxide layer on its surface.

APPENDICES

APPENDIX-A

A REVIEW OF SCHOTTKY BARRIER

When a metal and a simiconductor are brought into an intimate contact, a potential barrier arises, (a) because of the difference in thermionic work function of the semiconductor and metal or (b) from the existance of localized electron states on the surface of the semiconductor. The energy band relation at metal semiconductor contact is shown in Fig. A.1.

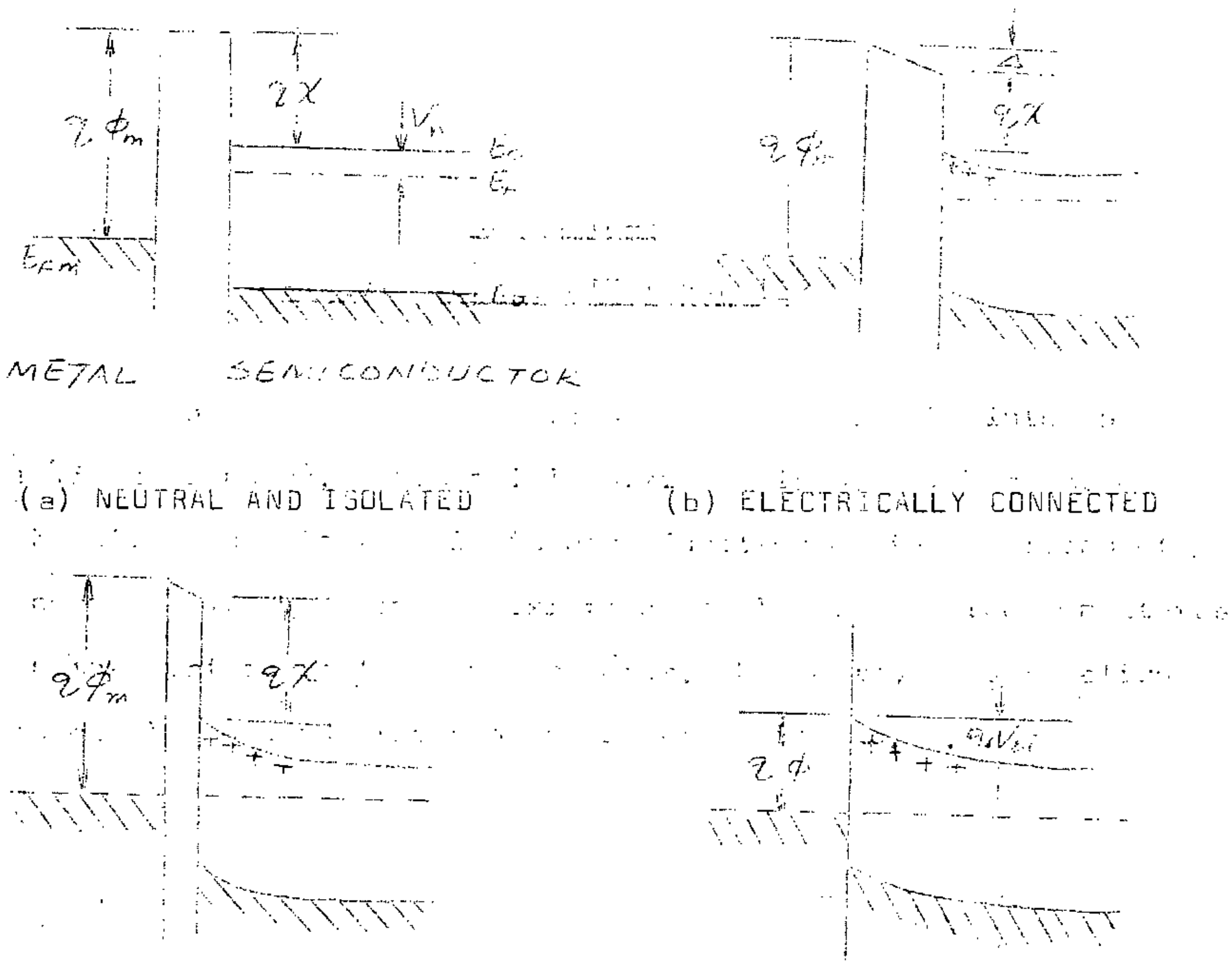

(a) NEUTRAL AND ISOLATED (b) ELECTRICALLY CONNECTED

(b) SEPERATED BY NARROW GAP (d) PERFECT CONTACT

FIGURE A.1 FORMATION OF SCHOTTKY BARRIER FROM METAL AND SEMICONDUCTOR.

Figure A.1(a) shows the relations at an ideal contact between a metal and an n-type semiconductor in the absence of surface states. If the semiconductor and metal are connected by a conducting wire, charge will flow from the semiconductor to the metal. Thus electronic equilibrium is established and Fermi levels on both sides come into coincidence. The Fermi level in the semiconductor is lowered by an amount equal to the difference between the two work functions, with respect to the Fermi level in the metal. This potential difference, $q\phi_m - q(\chi + V_n)$, is called contact potential where $q\chi$ is the electron affinity measured from the bottom of the conduction band to the vacuum level and qV_n is a measure of internal work function which is the difference between the Fermi level and the bottom of the conduction band. An electric field would then result in the gap because there must be negative charges on the metal side balanced by positive charges on the semi-conductor side. In the case of metals, large fields can be accounted for at a surface by only smaller variations of charge density. Hence a large field intensity may terminate at the metal surface in only a single lattice spacing or so. Because the concentration of donors is many order less in magnitude than the concentration of electrons depletion region occupy an appreciable thickness into the surface. In the metal, then, the abrupt termination of the field causes a break to appear in the potential curve, while in a semiconductor potential curve is smoother and the band in semiconductor is bent upward as shown in Fig. A.1(b).

As metal and semiconductor approach each other the drop in electrostatic potential (Δ) associated with the field gap tends to be zero if the field is to remain at a finite value. Finally when ∂ becomes small enough to be comparable with interatomic distances, the gap becomes transperent to electrons and the potential across the thin layer separating them disappears altogether leaving behind the barrier arising from band bending (Fig. A.1(d)).

Evidently the limiting value of the barrier height $q\phi_{Bn}$ (neglecting Schottky barrier lowering) is given by

$$q\phi_{Bn} = q(\phi_m - \chi) \qquad \text{A.1}$$

The semiconductor in Fig. A.1 possesses no net charge at the surface. It is, however, generally agreed that chemically etched semiconductor surfaces are covered with thin layers of oxides. Because of the mismatch of the crystallographic structures and dimension at the semiconductor oxide interface boundary, imperfactions in the structure are likely to exist and to create energy levels within forbidden gap. The extra energy levels created atsemiconductor surface are commonly called surface states. Bradeen[24] pointed out the effect of surface states on the height of the potential barrier. Surface states are usually continuously distributed in energy within forbidden band and are characterised by a neutral level $q\phi_o$ (which was the energy difference between the Fermi level and the valence band edge at the surface before the metal semi-conductor was formed). It specified the level below which all the surface states must be filled for the condition of neutrality of charge at the surface. When $q\phi_o > E_F$, there is a net positive charge at the surface states and the depletion region is not as wide as where there is no surface states and the barrier height is reduced. But if $q\phi_o < E_F$ there is a net negative charge at the surface states and the barrier height is increased.

In a p-type semiconductor the position is reverse and for ideal contact, the barrier height is given by

$$\phi_{Bp} = \frac{E_g}{q} - (\phi_m - \chi) \qquad A.2$$

Schottky barrier formation with surface states is shown in Fig. A.2 and a more detailed energy band diagram of a metal n-type semiconductor contact is shown in Fig.A.3.

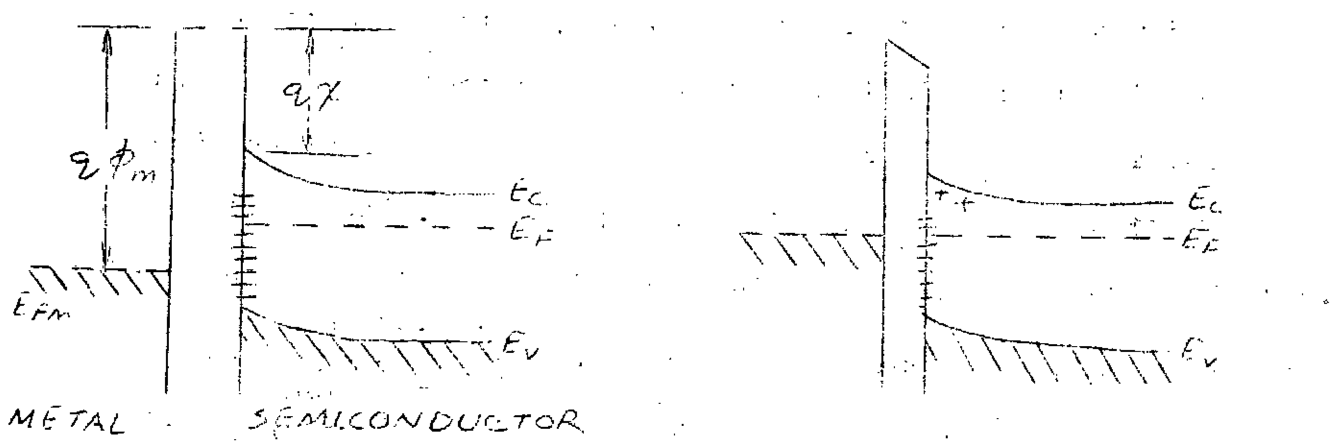

(a) NEUTRAL AND ISOLATED

(b) CONNECTED LECTRICALLY WITH THIN INTERFACIAL LAYER

FIGURE A.2 SCHOTTKY BARRIER FORMATION WITH SURFACE STATES.

the surface states must be filled for the condition of neutrality of charge at the surface. When a large density of surface states is present on the semiconductor surface a second Fig. A.2(a) shows the equilibrium between surface states and the bulk semiconductor.

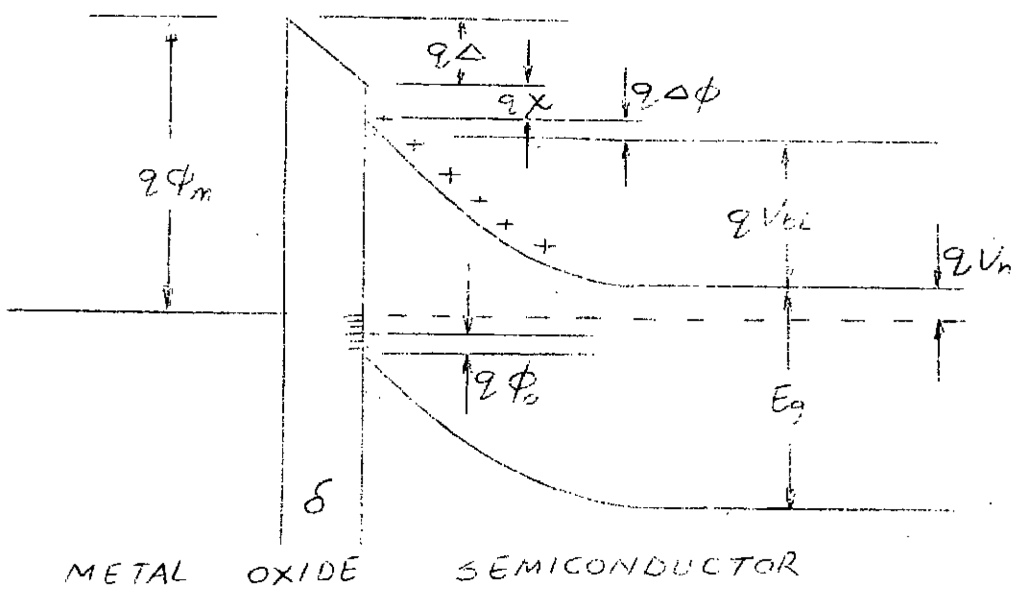

FIGURE A.3 ENERGY BAND DIAGRAM OF A METAL-n-TYPE SEMICONDUCTOR WITH AN OXIDE INTERFACIAL LAYER.

APPENDIX-B

CURRENT-VOLTAGE CHARACTERISTICS OF SOLAR CELLS

Current-voltage (I-V) characteristics for a solar cells can be obtained by three different methods.[67]

(1) Photovoltaic output characteristics:- This method applies a fixed illumination, usually of known intensity and a variable resistance load Fig. B.1. Voltage and currents are measured while the load resistance is varied.

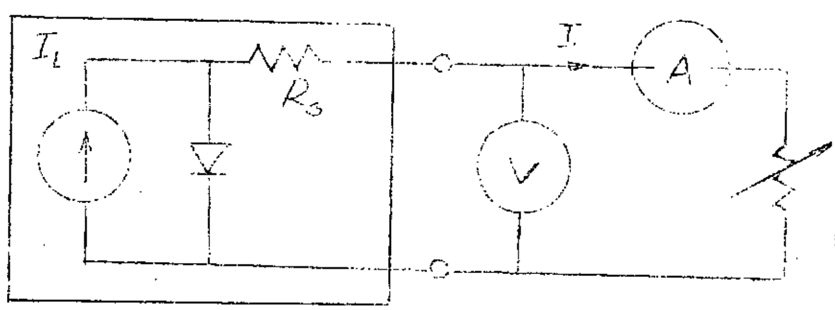

$$I = I_o \left\{ \exp \left[\frac{q}{nKT} (V - IR_s) \right] - 1 \right\} - I_L, \quad I \leqslant 0, \; V \geqslant 0$$

FIGURE B.1 PHOTOVOLTAIC OUTPUT CHARACTERISTICS (CONSTANT ILLUMINATION) MEASUREMENT

The current voltage characteristic thus obtained is known as 'photovoltaic output characteristic'.

(2) Diode forward characteristics:- This method tests the solar cell like a diode without application of any illumination. A dc power supply is used to obtain a current voltage characteristics as shown in Fig. B.2. The characteristic obtained by this method is known as 'diode forward characteristics'.

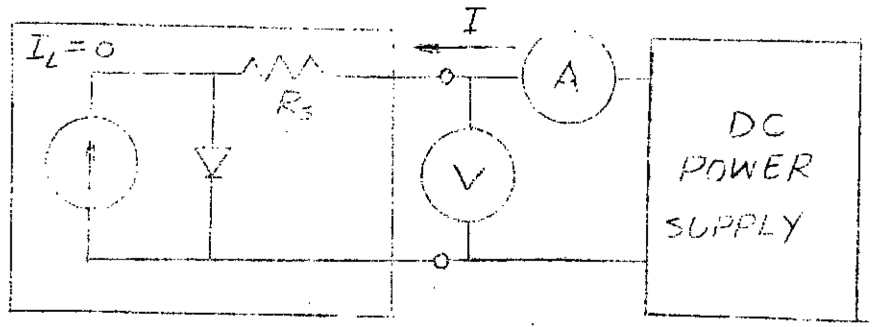

$$I = I_o \left\{ \exp\left[\frac{q}{nKT}(V - IR_s)\right] - 1 \right\}, \quad I \geqslant 0, \qquad V \geqslant 0$$

FIGURE B.2 DIODE FORWARD CHARACTERISTICS (WITHOUT ILLUMINATION) MEASUREMENT

(3) Junction characteristics:- In this method the solar cell is illuminated with a variable light intensity. The amount of illumination does not have to be known, if the value of light generated current I_L can be determined. The measuring circuit is shown in Fig. B.3.

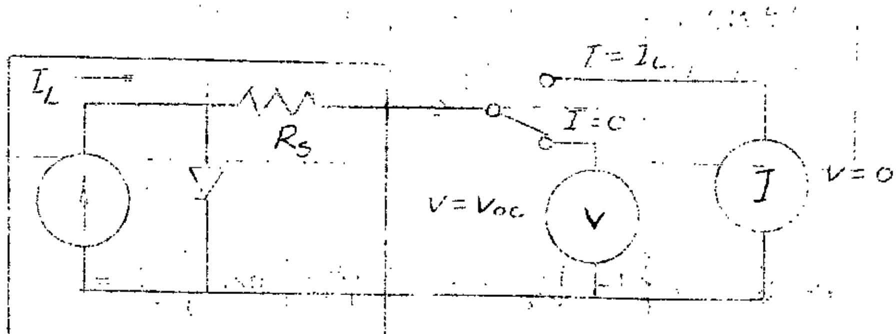

$$I_L = I_o \left[\exp\left(\frac{q V_{oc}}{nKT} \right) - 1 \right]$$

FIGURE B.3 JUNCTION CHARACTERISTICS (VARIABLE ILLUMINATION) (PLOT OF I_L Vs. V_{oc}). MEASUREMENT.

APPENDIX-C

The basic equation describing the I-V characteristic of a solar cell considering ehe effect of series resistance is

$$I = I_o \left(e^{B(V - IR_s)} - 1 \right) - I_L \qquad C.1$$

where $B = \frac{q}{nKT}$ and $V - IR_s = V'$ is the voltage across the junction which is larger than the terminal voltage V by the voltage drop in series resistance (Note that $I < 0$ for photovoltaic output characteristics) resulting in $V' > V$. for power generation in the solar cell (4th quadrant operation).

Introducing two light levels 1 and 2, one obtains two characteristics given by

$$I_1 = I_o (e^{BV_1'} - 1) - I_{L1} \qquad C.2$$

and

$$I_2 = I_o (e^{BV_2'} - 1) - I_{L2} \qquad C.3$$

Since V' is an independent variable, one can choose

$$V_1' = V_2' \qquad C.4$$

and can set $I_{L2} = I_{L1} + \Delta I_L$ C.5

and obtain.

$$I_2 = I_1 - \Delta I_L \qquad C.6$$

The equation $V' = V - IR_s$ C.7

however, results in two different terminal voltages V_1 and V_2 for two currents I_1 and I_2. From equation C.4, C.7, and C.6, follows

$$V_1 - I_1 R_s = V_2 - I_1 R_s + \triangle I_L R_s \qquad \text{C.8}$$

which describes a constant relationship between V_1 and V_2 for any choice of V_1. The constant of this relationship is proportional to the series resistance R_s and to the change of light intensity, Equation C.8 thus describes a second translation of the coordinate axis, this one parallel to the voltage axis by the amount

$$V_2 = V_1 - \triangle I_L R_s \qquad \text{C.9}$$

APPENDIX-D

A computer programme has been developed to find the equivalent circuit of the solar cells fabricated and based on this data the current and voltages at the maximum power points are calculated. Efficiency of the solar cell is also obtained at this maximum power point.

I-V characteristics of the cell is obtained in the dark condition. The internal series resistance is also measured as discussed in Chapter-4. With the help of this data the actual diode characteristic is obtained. The diode characteristics for higher value of voltages is approximated by

$$I = I_o \left(\exp\left(\frac{qV}{nKT}\right)\right) \qquad D.1$$

Taking natural logarithms on both sides

$$\log_e I = \log_e I_o + \left(\frac{q}{nKT}\right)V \qquad D.2$$

The data for the diode at higher values is approximated by a straight line using least-square error method by the following equation

$$Y = a_1 + a_2 V \qquad D.3$$

From these results we have

$$I = e^{a_1} \quad \text{and} \quad n = \frac{1}{a_2}\left(\frac{q}{KT}\right) \qquad D.4$$

After obtaining the diode equation the photogenerated current is obtained by using the value of short circuit current and the following equation

$$I_L = I_o \left(\exp \left(\frac{q}{nKT} \left(I_{sc} R_s \right) - 1 \right) \right) + I_{sc} \qquad D.5$$

The maximum power point is obtained by solving

$$I = I_L - I_o \left(\exp \left(\frac{q}{nKT} \left(I(R_s + R_L) \right) - 1 \right) \right) \qquad D.6$$

for different values of load resistance R_L. From the knowledge of area of the solar cell, power input density the efficiency of the solar cell, the fill factor is obtained.

The computer programme, run on BUET IBM 370/115 computer, is given in the next page.

```
C     DETERMINATION OF THE COEFFICIENTS OF THE POLYNOMIAL
C     V(I)=VOLTAGE POINTS,AI(I)=CURRENTS,C(I,J)=MATRIX FOR LEAST-SQUARE CURVE
C     FITTING,B(I,J)=C(I,J),U(I,J)=DESIRED UNIT MATRIX,K(I)=COEFFICIENT MATRIX
C     N=NO. OF DATA POINTS.  M=DEGREE OF POLYNOMIAL
C     V(I) IN MILLIVOLTS, AI(I) IN MICROAMPERES.
      DOUBLE PRECISION V(10),AI(10),C(7,7),B(7,7),U(7,7),D(7),AK(7),BB(7
     1,7),CC(7,7),P(7),AL,RS,RLI,PIN,RL,AI1,X,CB,AVI,AA,EFF,AN,AII(7,7),
     1AP,Y,YN,ANO,VOC
      READ(1,50) N,M
   50 FORMAT(2I2)
      WRITE(3,653) N,M
  653 FORMAT(//20X,'N='I2,40X,'M='I2//)
 6666 READ(1,51) (V(I),I=1,N),(AI(I),I=1,N)
      WRITE(3,52) (V(I),I=1,N)
      WRITE(3,52) (AI(I),I=1,N)
   52 FORMAT(//10X,7D15.5/)
 5555 READ(1,600) AL,RS,RLI,PIN,AREA,ACREA
  600 FORMAT(6D10.3)
      WRITE(3,5556) AL,RS,RLI,PIN,AREA,ACREA
 5556 FORMAT(24X,'AL='D10.3,2X,'RS='D10.3,2X,'RLI='D10.3,2X,'PIN='D10.3,
     1 2X,'AREA='D10.3,'ACREA='D10.3/)
      DO 748 I=1,N
  748 V(I)=V(I)-AI(I)*RS*1.D-03
      DO 747 I=1,N
  747 AI(I)=DLOG(AI(I))
      WRITE(3,52) (V(I),I=1,N)
      WRITE(3,52) (AI(I),I=1,N)
   51 FORMAT(8D10.5)
      DO 707 J=1,M
      C(M,J)=0.0
  707 C(1,J)=0.0
      C(1,1)=N
      DO 20 I=1,M
   20 D(I)=0.0
      M2=M-2
      DO 10 J=1,M
      X=J-1
      Y=J+M2
      DO 10 I=1,N
      IF(X) 400,400,401
  400 D(1)=D(1)+AI(I)
      GO TO 10
  401 D(J)=D(J)+AI(I)*(V(I)**X)
   55 C(1,J)=C(1,J)+V(I)**X
      C(M,J)=C(M,J)+V(I)**Y
   10 CONTINUE
      C(M,1)=C(1,M)
      M1=M-1
      DO 13 I=2,M1
      DO 13 J=1,M
      IF(J-M) 120,21,21
  120 C(I,J)=C(I-1,J+1)
      GO TO 13
   21 C(I,J)=C(J,I)
```

```
   13 CONTINUE
      WRITE(3,3)
    3 FORMAT(//55X,'FORMED MATRIX-C(I,J)'/)
      WRITE(3,1)((I,J,C(I,J),J=1,M),I=1,M)
    1 FORMAT(/5(5X,'C('I1,',',I1,')='D12.5))
      WRITE(3,604)
  604 FORMAT(//55X,'FORMED MATRIX-D(I)'/)
      WRITE(3,2)(I,D(I),I=1,M)
    2 FORMAT(/5(1X,'D('I1,')='D12.5))
      P(1)=0.0
      DO 15 I=1,4
   15 P(1)=P(1)+C(I,I)
      DO 16 I=1,4
      DO 16 J=1,4
   16 CC(I,J)=C(I,J)
      DO 17 K=2,4
      DO 18 I=1,M
      DO 18 J=1,M
   18 BB(I,J)=CC(I,J)
      DO 19 I=1,4
   19 BB(I,I)=BB(I,I)-P(K-1)
      DO 920 I=1,M
      DO 920 J=1,M
      CC(I,J)=0.0
      DO 920 L=1,M
  920 CC(I,J)=CC(I,J)+C(I,L)*BB(L,J)
      Q=0.0
      DO 921 I=1,M
  921 Q=Q+CC(I,I)
      R=K
   17 P(K)=Q/R
      DO 23 I=1,4
      DO 23 J=1,4
   23 AII(I,J)=BB(I,J)/P(M)
      WRITE(3,6)
    6 FORMAT(/55X,'INVERSE MATRIX-AII(I,J)'/)
      WRITE(3,222) ((AII(I,J),J=1,M),I=1,M)
  222 FORMAT(1X,6D20.8)
      DO 101 I=1,M
      DO 101 J=1,M
  101 U(I,J)=0.0
      DO 100 I=1,M
      DO 100 J=1,M
      DO 100 K=1,M
  100 U(I,J)=U(I,J)+C(I,K)*AII(K,J)
      WRITE(3,605)
  605 FORMAT(/52X,'DESIRED MATRIX-U(I,J)'/)
      WRITE(3,223)((U(I,J),J=1,M),I=1,M)
  223 FORMAT(//45X,2D20.5)
      DO 555 I=1,M
  555 AK(I)=0.0
      DO 500 I=1,M
      DO 500 K=1,M
  500 AK(I)=AK(I)+(AII(I,K)*D(K))
```

```
      WRITE(3,77)(I,AK(I),I=1,M)
      WRITE(3,667)
   77 FORMAT(//5X,6('AK('I2,')='D12.5,1X))
      AO=DEXP(AK(1))
      AN=1./(26.*AK(2))
      PHIB=.026*DLOG(AREA*32.*(300**2)/(AO*1.D-06))
C     SOLUTION FOR MAX. POWER OUTPUT OF SOLAR CELL
C     AL=PHOTOGENERATED CURRENT,AO=DARK SATURATION CURRENT
C     AN=IDEALITY PARAMETER,RS=SERIES RESISTANCE,PIN=INPUT POWER/SQ.CM
      AL=AL+AO*(DEXP((AL*RS)/(AN*26000.))-1.0)
      WRITE(3,667)
      WRITE(3,8888) AL,PHIB
 8888 FORMAT(32X,'PHOTOGENERATED CURRENT='D10.5,4X,'BARRIER HEIGHT='D10.
     15,'EV')
      VOC=(DLOG(AL/AO))/AK(2)
      WRITE(3,710) AO,VOC
  710 FORMAT(25X,'DARK SATURATION CURRENT AO='D10.5,5X,'OPEN CIRCUIT VOL
     1TAGE VOC='D10.5)
C     CALCULATION OF CURRENT AT MAXIMUM POWER
  667 FORMAT(1X,131('-'))
      WRITE(3,667)
      WRITE(3,666)
  666 FORMAT(23X,'CURRENT',11X,'RESISTANCE',13X,'POWER'12X,'EFFICIENCY'
     1,12X,' VOLTAGE'/)
      WRITE(3,667)
    6 RL=0.0
    7 AI1=0.0
      Y=0.0
      X=AI1-AL+AO*(DEXP(AI1*(RS+RL)/(AN*26000.))-1.0)
      IF(Y.EQ.0.0) GO TO 800
      IF(DABS(X).GT.DABS(Y)) GO TO 801
  800 Y=X
      AVI=AI1
  801 AI1=AI1+5.
      IF(AI1.LT.AL) GO TO 7777
      AA=(AVI/10**6)
      AP=(AA**2)*RL
      VOL=AA*RL
      EFF=(AP/(PIN*AREA))*100.
      WRITE(3,802) AVI,RL,AP, EFF,VOL
  802 FORMAT(15X,5D20.8)
      RL=RL+10
      IF(RL.LE.RLI) GO TO 7
      GO TO 6666
  610 CALL EXIT
      END
```

BIBLIOGRAPHY

1. Smits, F.M. "History of Silicon Solar Cells", IEEE Trans., Electron Devices, Vol. ED-23, No.7, July 1976, pp 640-643.

2. Cummerow, R.L. "Photovoltaic Effect in p-n Junction", Physical Review, Vol. 95, pp. 16-21, July, 1954.

3. Cummerow, R.L. "Use of p-n Junction for Converting Solar Energy to Electrical Energy", Phys. Rev., Vol. 95, pp 561-562, July 1954.

4. Rittner, E.S. "Use of p-n Junction for Solar Energy Conversion", Phys. Rev., Vol. 96, pp 1708-1709, Dec. 1954.

5. Gremmelmair, R. "GaAs-Photoelement", Z. Naturforschg, Vol. 10a, pp 501-502, 1955.

6. Prince, M.B. "Silicon Solar Energy Converters", J. Appl. Phys. Vol. 26, pp. 534-540, May 1955.

7. Lofersky, J.J. "Theoretical Considerations Governing the Choise of the Optimum Semiconductor for Photovoltaic Solar Energy Conversion", J. Appl. Phys. Vol. 27, pp. 777-784, July 1956.

8. Jenny, D.A. "Photovoltaic Effect in GaAs p-n Junction and Solar Energy Conversion", Phys. Rev. Vol. 101, pp. 1208-1209, Feb. 1956.

9. Rappaport, P. and Loferski, J.J. "New Solar Converter Materials", Proc. of 11th Annual Battery R and D Conference (U.S. Army signal Engg. Lab., Fort, Monmouth, NJ, May 1957, pp. 96-99.

10. Pearson, G.L. "Conversion of Solar Energy to Electrical Energy", American Journal of Physics, Vol. 25, pp. 591-598, Dec. 1957.

11. Loferski, J.J and Rappaport, P. "The Effect of Radiation on Silicon Solar Energy Converters", RCA, Rev., Vol. 19, pp 536-554, Dec. 1958.

12. Rosenzweig, W., Smits, F.M., and Brown, W.L. "Energy Dependence of Proton Irradiation Damage in Silicon", J. Appl. Phys., Vol. 35, pp. 2707-2711, 1964.

13. Denney, J.M., and Downing, R.G. "Proton Radiation Damage in Silicon Solar Cells", TRW System Reports, 8653-6026, KV-000, 1963.

14. Rosenzweig, W., Gummel, H.K. and Smits, F.M. "Solar Cell Degradation under 1 Mev Electron Bombard", Bell Syst. Tech., Journal, Vol. 42, pp 399-414, 1963.

15. Childester, L.G, "Progress Report — Space Station Solar Array Program", Proc. of 7th Intersociety Energy Conversion Engineering Conference", pp. 409-419, Sept. 1972.

16. Lindmayer, J. and Allison, J.F. "Violet Cells: An Improved Silicon Solar Cells", COMSAT, Tech. Rev. Vol. 3, pp 1-22, 1973.

17. Haynon, et al "The COMSAT Nonreflective Silicon Solar Cells", Proc. International Conference Photovoltaic Power Generation (Germany) pp 487-500, Sept. 1974.

18. Braun, F. Am. Physik Chem, Vol. 153, pp 556-562.

19. Pickard, G.W. U.S. Patent No. 836531, 1906.

20. Pierce, G.W. Phys. Rev., Vol. 25, pp 31-32, 1907.

21. Wilson, A.H. Proc. Royal Society, A 133, p. 458, 1931.

22. Schottky, W Natarwiss, Vol. 26, pp. 843-853, 1938.

23. Mott, N.F. "Notes on Contact Between a Metal and an Insulator or Semiconductor", Proc. Comb. Phil. Soc., 34, p 568, 1938.

24. Bardeen, J. "Surface States and Rectification at a Metal Semiconductor Contact", Phys. Rev. Vol. 71, pp 717-727, 1947.

25. Archer, R.T. and Atalla Am. N.Y. Acad. Sci., 101, p. 697, 1963.

26. Goodman, A.N.M. J. App. Phys., Vol. 34, No.2, pp.329, 1963.

27. Cowley, A.M. and Sze, S.M. "Surface States and Barrier Height of Metal Semiconductor System", J. Appl. Phys., Vol. 36, pp. 3212-3220, 1965.

28. Crowell, C.R. "The Richardson Constant for Thermionic Emission in Schottky Barrier Diode", Solid State Electronics, Vol. 18, pp.395-399, 1965.

29. Crowell, C.R. and Sze. S.M. "Current Transport Theory in Metal Semiconductor Barriers", Solid State Electron., Vol. 19, pp. 1035-1048, 1966.

30. Mead, C.A, "Metal Semiconductor Surface Barriers", Solid State Electron., Vol. 9, pp. 1023-1033, 1966.

31. Turner, M.J. and Rhoderick, E.H. "Metal Silicon Schottky Barrier", Solid State Electron., Vol.11, pp 291-300, 1968.

32. Smith, B.L. and Rhoderick, E.H. "Schottky Barrier on p-type Silicon", Solid State Electron. Vol. 14, pp 71-75, 1971.

33. Croweld, C.R. and Beguwala, M. "Recombination Velocity Effect on Current Diffusion and Imref in Schottky Barrier", Solid State Electron. Vol. 14, p-1149, 1971.

34. Card, H.C and Rhoderick, E.H. "Studies of Tunnel MOS Diodes I. Interface Effects in Silicon Schottky Diodes", J. Phys. D, Appl. phys., Vol.4, pp 1589-1601, 1971.

35. Card, H.C., and Rhoderick, E.H. "Studies of Tunnel Mos Diodes, II. Thermal Equilibrium Considerations", J. Phys. D., Appl. Phys. Vol.4, pp 1602-1611, 1971.

36. Patwari, A.M. and Hartnagel, H.L. "Effect of Surface Properties on n-Type GaAs-Ni and GaAS-Al Schottky Diodes", Phys. Stat. Sol. (a) 26, 469, 1974, Department of Electrical and Electronic Engineering, Merz Laboratories, University of New Castle Upon Tyne.

37. Alam, Md. S. "An Investigation into some Metal-Silicon Schottky Barrier Diodes", M.Sc.Engg. Thesis, Deptt. of Electrical Engineering, BUET, 1978.

38. Anderson, W.A., and Delahoy, A.E. "Schottky Barrier Diodes for Energy Confersion", Proc. IEEE, 1972, Vol.60, pp 1457-1458.

39. Anderson, W.A. and Delahoy, A.E. "Advances in Schottky Barrier Solar Cell Technology", Proc. 8th IECEC, 1973, August, pp 326-330.

40. Green, M.A., King, F.D. and Shewchun, J "Minority Carrier MIS Tunnel Diodes and Their Application to Electron-and Photo-voltaic Energy Converston, - I, Theory", Solid State Electronics, 1974, Vol.17, p.551.

41. Pulfrey, D.L and McQuat, R.F. "Schottky Barrier Solar Cell Calculation", Appl. Phys. Letts. Vol. 24, No.4, Feb. 1974.

42. Anderson, W.A., Delahoy, A.E. and Milano, R.A. "An 8% Efficient Layered Schottky Barrier Solar Cell", Journal of App. Phys. Vol.45, No.9, Sept. 1974.

43. Anderson, W.A., Milano, R.A. "I-V Characteristics for Schottky Barrier Solar Cells", Proc. IEEE, Jan, 1975, pp 206-208.

44. Fonash, S.J. "The Role of the Interfacial Layer in Metal Semiconductor Solar Cells", J. Appl. Phys. Vol. 46, No.3, March 1975.

45. Stirn R.J. and Yeh, Y.C.M. "A 15% Efficient Antireflection Coated Metal-Oxide-Semiconductor Solar Cell", Appl. Phys. Letts, Vol27, No.2, 15 July, 1975.

46. Charlson, E.J., and Lien J.C. "An Al-p-Silicon MOS Photovoltaic Cell" J. App. Phys. Vol. 46, No.9, Sept., 1975, pp. 3982-3987.

47. Lillington, D.R. and Townsend, W.G. "Effects of Interfacial Layer on the Performance of Silicon Schottky Barrier Solar Cells", Appl. Phys. Letts. Vol.28, No.2, 15 Jan. 1976, pp. 97-98.

48. Pulfrey, D.L. "Barrier Height Enhancement in P-Silicon MIS Solar Cells", IEEE Trans. On Electron Devices, June, 1976, pp 587-589.

49. Card, H.C. and Yang, E.S. "MIS Schottky Theory under Conditions of Optical Carrier Generation in Solar Cells", Appl. Phys. Letts, Vol.29, No.1, July 1976, pp. 51-53.

50. Anderson, W.A., Vernon, S.M., Mathe, P. and Lelevic, B. "Schottky Solar Cells on Thin Epitaxial Silicon", Solid State Electronics, 1976, Vol. 19, p. 973.

51. Anderson, W.A., Kim, J.K., and Delahoy, A.E. "Barrier Height Modification in Silicon Schottky (MIS) Solar Cells", IEEE Trans. on Electron Devices, Vol. ED-24, No.4, pp. 453-457, April 1977.

52. Li, Sheng, S. "Theoretical Analysis of a Novel MPN Galium Arsenide Schottky Barrier Solar Cell", Solid State Electron. 1978, Vol.21, pp 435-438.

53. Anderson, W.A., Delahoy, A.E., Kim, J.K. and Hyland, S.H. "High Efficiency Cr- MIS - Solar Cells on Single and Polycrystalline Silicon", Appl. Phys. Letts, 33(7), 1 Oct. 1978, pp. 588-590.

54. Lue, J.T. and Hong, Y.D. "The Dependence of the Photocurrent of the MIS Solar Cells on Thickness of Schottky Barrier Metals", Solid State Electron., Vol. 21, 1978, pp.1213-1218.

55. Fuchs, K. Proceedings Cambridge Phil. Soc., 34, 100, 1938.

56. Sondheimer, F.H. Advanced Physics, 1, 1(1952).

57. Handy, R.J. "Theoretical Analysis of the Series Resistance of A Solar Cell", Solid State Electron., 10, pp.765-775, 1967.

58. Pulfrey, D.L. "On the Fillfactor of Solarcells", Solid State Electron., 1978, Vol.21, pp. 519-520.

59. Pulfrey, D.L. "MIS Solar Cells: A Review", IEEE Trans., on Electron Devices, Vol. ED-25, No.11, Nov. 1978.

60. Rajkanan, K, and Anderson, W.A. "Current Conduction in Cr-MIS Solar Cells on Single Crystal P-Silicon", Appl. phys. Letts, 35(5) 1 Sept., 1979.

61. RajKannan, K, Sing, R. and Shewchun, J. "Open Circuit Voltage and Interface Study of Silicon MOS Solar Cells", IEEE Trans. on Electron Devices, Vol.ED-27, No.1, Jan. 1980.

62. RajKannan, K and Shewchun, J. "A Better Approach to the Evaluation of the Series Resistance of Solar Cells", Solid State Electron., Feb. 1979, pp. 193-197.

63. Gartner, W.W. Phys. Rev., 116, 84, 1959.

64. Landsberg, P.T. and Klimpke, C. Proc. R. Soc. Lond. A 354, 101-118, 1977.

65. Harrison, W.A. Physical Rev., 1961, 123, 85-89.

66. Gray, P.V., "Tunneling from Metal to Semiconductor", Physical Rev, Sept.-Oct. 1965, 140, A 179-186.

67. Wolf, M. and Rauschenbach, H. "Series Resistance Effects on Solar Cell Measurements", Adv. Energy Conv. Vol.3, Apr.-June, 1963.

68. Angrist, S.W. Direct Energy Conversion, Allyn and Becon, Inc., Boston, 1965.